UC/CLC CAMPUS EARTHQUAKE PROGRAM

Initial Source and Site Characterization Studies for the U.C. Riverside Campus

Stephen K. Park
Scott Elrick
Richard Funk

Institute of Geophysics and Planetary Physics

University of California, Riverside

July, 1999

UCRL-ID-134610

PREFACE

This report was prepared under the UC/CLC Campus Earthquake Program (CEP), which was initiated as part of the Campus-Laboratory Collaboration (CLC) Program created by the University of California Office of the President (UCOP).

The Campus Earthquake Program started in March 1996 as a partnership between four campuses of the University of California - Los Angeles, Riverside, Santa Barbara, and San Diego - and the Lawrence Livermore National Laboratory (LLNL). In 1998, three additional UC campuses - Berkeley, Davis, and Santa Cruz - were added to the collaboration. The current CEP studies focus on Riverside, San Diego, and Santa Barbara. Each campus has selected a critical site to demonstrate the methods and procedures used by the CEP. The following sites have been selected: the Rivera Library at UC Riverside, the Thornton Hospital at UC San Diego, and the Engineering 1 building at UC Santa Barbara.

In the first phase of the program, March 1996 - April 2000, we are estimating strong ground motions at each critical site. These estimates are obtained by using an integrated geological, seismological, geophysical, and geotechnical approach, bringing together the unique capabilities of the campus and laboratory personnel. This program is also designed to maximize student participation. Many of the site-specific results are also applicable to risk evaluation of other sites on the respective campuses. In the next phase, the program is planning to extend the integrated studies of strong ground motion effects to other interested UC campuses which are potentially at risk from damaging earthquakes. At UC Riverside, the current phase also involves the study of ground motion at future building sites in order to guide structural engineers in the design phase for those buildings.

This report describes the initial seismic source and site characterization studies performed for the UC Riverside campus where a new seismic station has been installed. The Principal Investigator (PI) at Riverside is Professor Stephen Park.

The Campus Earthquake Program is funded from several additional sources, which leverage the core support provided by the Office of the President and which are gratefully acknowledged. These sources included the University Relations Program at LLNL, directed by Dr. Claire Max, and the offices of the appropriate Vice-Chancellors on the various campuses. At UC Riverside, the Vice-Chancellor for Administration is Michael Webster.

The Director of the UC/CLC Campus Earthquake Program is Dr. Francois Heuze from LLNL.

TABLE OF CONTENTS

EXECUTIVE SUMMARY

With its proximity to faults capable of generating large earthquakes within our lifetimes, good assessment of potential ground motions on the University of California, Riverside campus is essential. A collaborative project led by Lawrence Livermore National Laboratory with participants from several UC campuses is developing a new methodology for assessing these ground motions. This approach involves characterization of the geotechnical properties of the geologic units on campus, monitoring of small local earthquakes at depth and at the surface, and computer modeling to generate strong motion estimates for large earthquakes. The first step in this project was to identify faults that could produce moderate to strong ground motion at UCR. These are:

San Andreas fault zone	M 7.6-8.1
San Jacinto fault zone	M 6.7-7.6
Elsinore fault zone	M 6.8-7.2
Cucamonga fault zone	M 7.3

The second step in this project was to characterize the geologic environment of the campus. Our geophysical studies of the UCR campus have revealed that the campus sits on 90-150 m thick alluvial sediments overlying granitic basement. Because the seismic wave (shear) velocities decrease rapidly towards the surface (from nearly 800 m/s at 30 m depth to under 200 m/s at the surface), substantial amplification of the seismic waves is expected. Observations of two recent earthquakes with a new triaxial borehole accelerometer array at the Rivera Library site reveal that peak accelerations are amplified by a factor of 10 for weak motions there. For strong motions,

the actual amplification will depend on the nonlinear properties of the soils and their condition of water saturation. This is why we have performed detailed in-situ and laboratory tests of the main soil types at the Riverside campus. Modeling based on observed weak ground motions, soil properties, and geology will result in site-specific estimates of strong ground motions at the Rivera site.

Continuing seismic monitoring at 5 more sites on campus will provide new weak motion records. At two of these locations, we will perform drilling to bedrock and in-situ measurements of soil properties. This will permit strong ground motion estimates to be made for two of these additional sites. With the addition of more limited near-surface geotechnical data and depth to bedrock inferred from geophysical measurements, estimates of surface motions at the three other sites on campus can be interpolated from the responses at the Rivera Library and the other two sites with drillholes to bedrock.

LIST OF FIGURES

Page

LIST OF TABLES

Page

1.0 INTRODUCTION

1.1 Methods and Philosophy of the CLC Campus Earthquake Program

The CLC Program, "Estimating of Ground Motion Exposure at Three UC Campuses in Southern California", is a 4-year effort involving the Lawrence Livermore National Laboratory (LLNL) and 7 UC campuses. The purpose of this project is to estimate ground motions from large earthquakes by combining techniques from geology, seismology, soil dynamics, and earthquake engineering into a single integrated approach. A single structure has been identified at each campus for detailed study; officials from Planning, Design and Construction have selected Rivera Library at UCR. The observed ground motion at UCR is the result of several factors: the magnitude, duration, and location of the earthquake; the modification of the seismic waves by propagation from the source to bedrock beneath the campus; and the modification of the seismic waves as they propagate up from the bedrock to the surface. The CLC program relies on the studies by SCEC (Jackson et al., 1995) for the first factor. Typically, the second factor is included through the use of empirical curves which relate ground acceleration to the distance and magnitude of an earthquake (Boore et al., 1993). While suitable for regional studies, these attenuation relations have large uncertainties that make them questionable for detailed site studies. Instead, the CLC project will develop its own estimates specific to each campus, based on earthquake records obtained on the campus itself.

The final factor, modification of the ground motion caused by seismic waves as they propagate upward through the soil column, is estimated using models of wave propagation in soils with nonlinear stress-strain properties. For weak motions, these models use mainly soil

properties determined from in-situ geophysical logging, and they are validated using earthquakes recorded at bedrock and at the surface at the site. For strong motions, they use nonlinear soil properties obtained from laboratory tests on samples recovered from boreholes at the site. The modification of the seismic waves by the soil column can result in extreme small scale variability, as observed with the 1994 Northridge earthquake (Hough and Field, 1996). Factors of 2 in ground motion amplitude are observed over distances of 500-1000 m, indicating that the most reliable method of predicting the modification by the soil column is through the use of observed records and modeling of local soil conditions based on measured physical properties. The ultimate goal of the CLC project is to predict the effect of ground motions from moderate to strong earthquakes through the integrated process described above.

1.2 Seismic Hazards in California

California sits atop the margin between the North American and Pacific plates. As these two plates slide past one another, earthquakes occur on a system of faults throughout the state. The best known feature of this plate interaction is the San Andreas fault, but many other faults contribute to the seismic hazard (Figure 1). All of the southern UC campuses are within 20 km of faults capable of generating moderate to large earthquakes. Indeed, movement on each of these faults has generated such earthquakes in the historic past. As a result, the exposure of these campuses to seismic hazards is very substantial.

The Southern California Earthquake Center (SCEC) has a continuing research program to understand the regional tectonics of southern California and to estimate seismic hazards in the region. A major effort of this center has been to identify and characterize potential earthquake

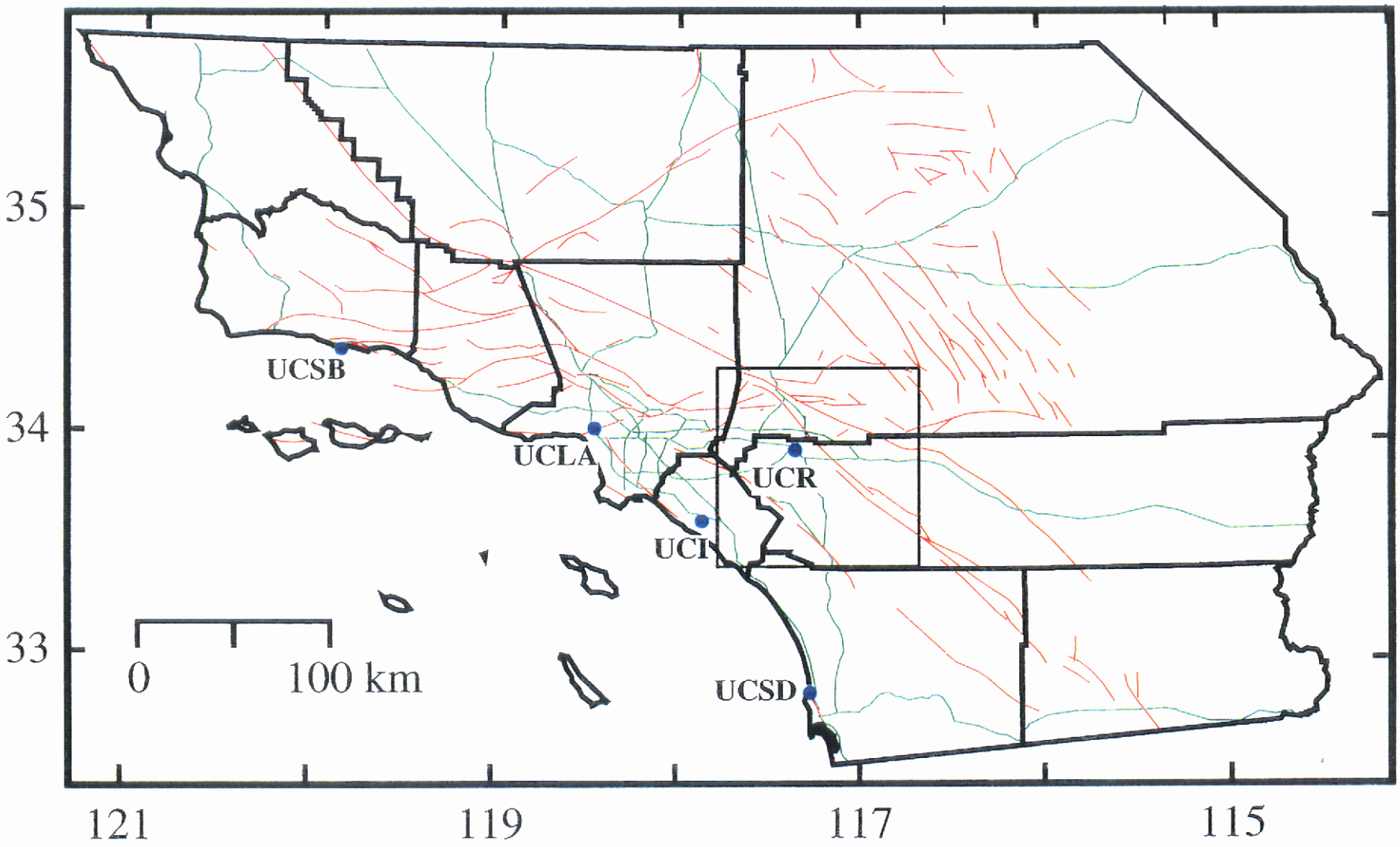

Figure 1 - Location map for southern California showing active faults (red), road network (green), county boundaries (black), and U.C. campuses (blue).

sources (i.e., faults) in southern California. Previous efforts have focused primarily on the mapped surface faults and have relied on geologic studies of individual faults (Wesnousky, 1986; WCGEP, 1988). SCEC has advanced the state-of-the-art by incorporating ground deformation studies, buried faults, and regional seismicity into models of seismic sources (Jackson et al., 1995). Many of the earthquakes in southern California do not lie on mapped surface faults (Figure 2), but these regions still contribute potential seismic sources and must be included in complete models of seismic hazards. Seismic hazards are typically estimated as a probability that a particular location will experience ground acceleration above a specified level within a specified period. This definition of seismic hazard permits the inclusion of multiple sources (faults) in the estimation of the hazard at a single point. The regional map of seismic hazard for southern California (Figure 3) shows that UCR falls within one of the most hazardous regions, with a probability greater than 60% that the campus will experience peak ground accelerations exceeding 0.2g in the next 30 years (Jackson et al., 1995).

1.3 Seismic Hazard Exposure at UCR

UC Riverside sits in close proximity to 3 major southern California faults (Figure 1), which leads to its high probabilities of experiencing peak horizontal accelerations of 0.2g or greater in the next 30 years. Structural engineering studies of campus buildings have revealed that several have a significant seismic risk. Degenkolb and Associates (1978) identified 4 buildings on campus which would have Very Poor seismic performance (Figure 4). A Very Poor ranking meant that extensive structural damage and high risk to life could be anticipated in a major earthquake (Degenkolb and Associates, 1978). All four of these buildings, the Bell Tower, the

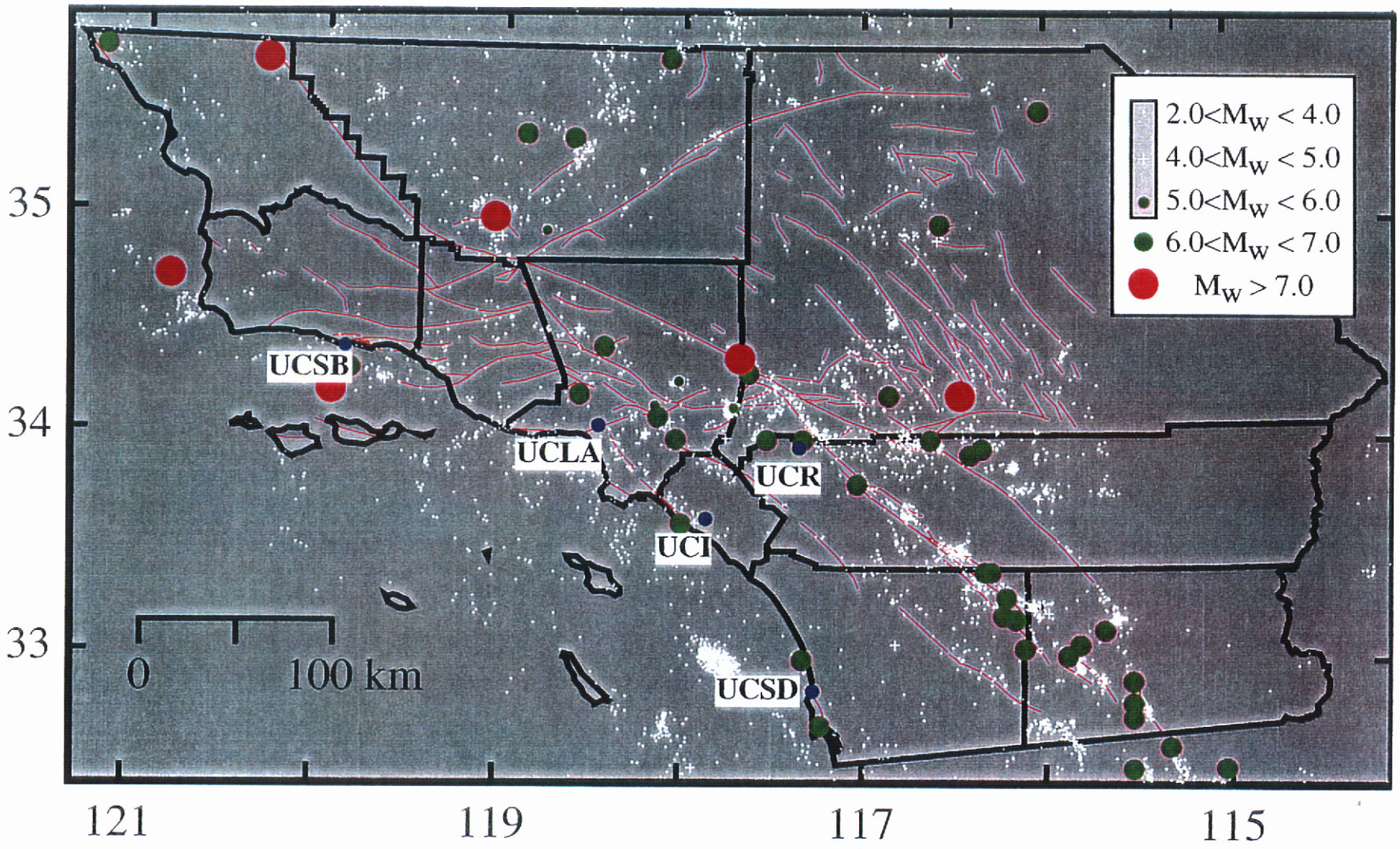

Figure 2 - Map showing distribution of earthquakes in southern California. Mw < 6.0 earthquakes are plotted from 1988 to 1991 (SCEC Data Center). Mw > 6.0 earthquakes are plotted from 1769 to 1992 (Ellsworth, 1990; Jackson, 1995). Note that many earthquakes do not fall on mapped faults.

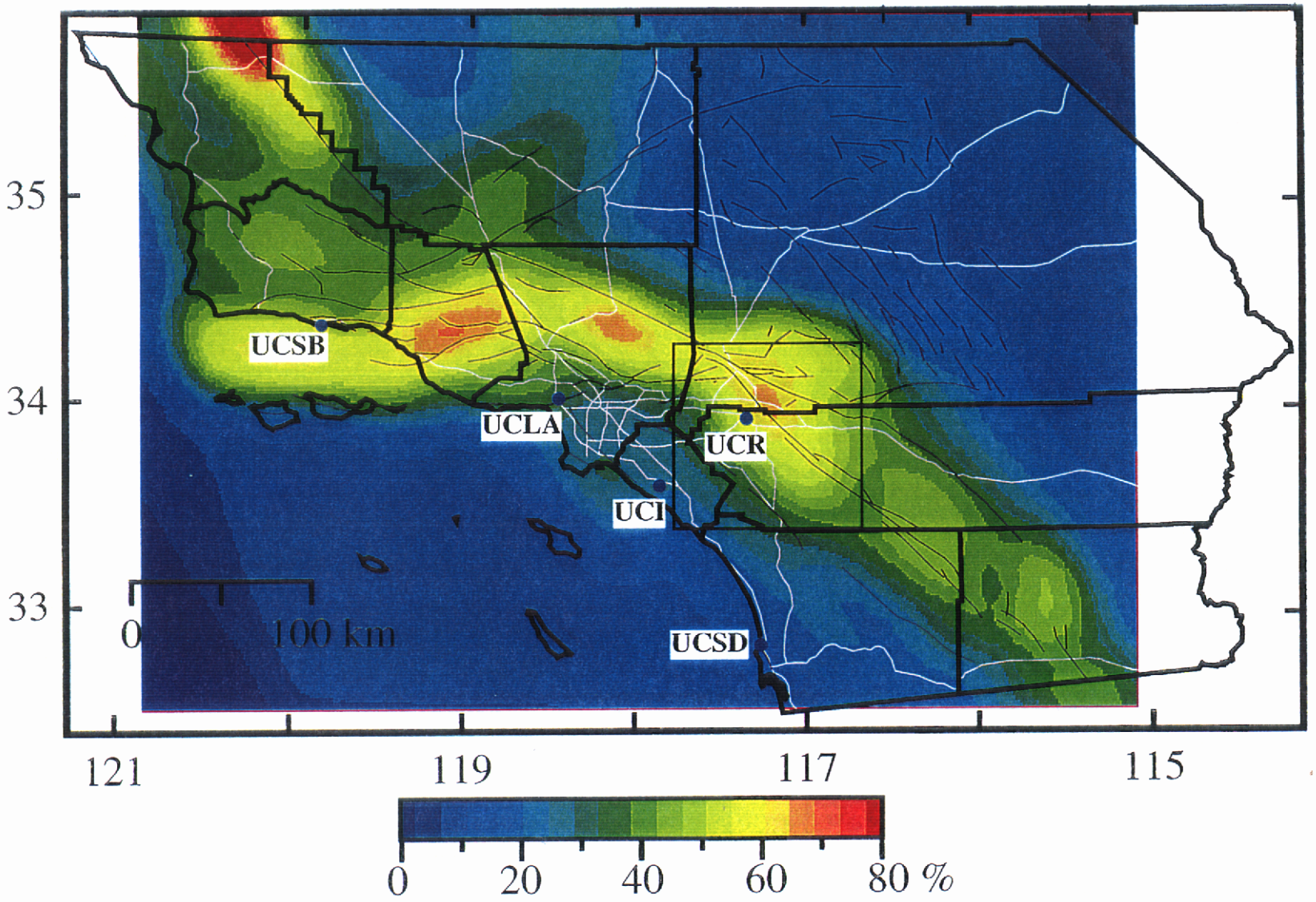

Figure 3 - Probability of 0.2 g horizontal acceleration on rock in the next 30 years (modified from Jackson et al, 1995).

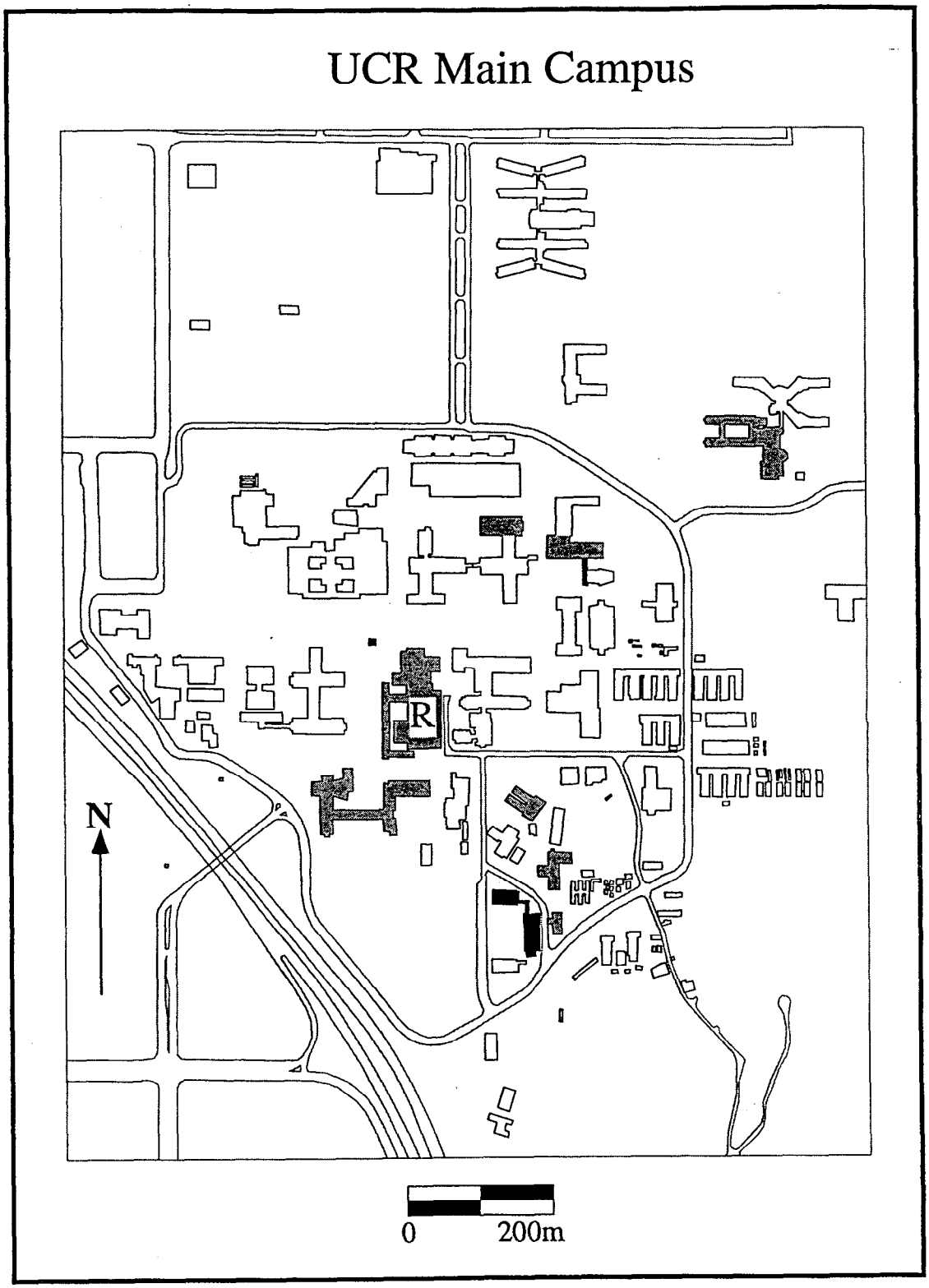

Figure 4 - Map of the UCR campus with buildings rated as "Very Poor" (dark grey) or "Poor"(light grey). All "Very Poor" buildings have been seismically upgraded, as well as some "Poor" buildings. The Rivera Library is marked with an "R".

Anderson School of Management (formerly Soils and Plant Nutrition 1 and 2), and the Physics colonnade, have been seismically retrofitted subsequent to this 1978 report. Additionally, 9 buildings were ranked with a Poor seismic performance (Figure 4). This ranking meant that significant structural damage and appreciable life hazard could be anticipated (Degenkolb and Associates, 1978). Plans are currently underway to retrofit these buildings. One of the buildings with a Poor ranking in this study was Rivera Libary because of the additions to it. This 5-story building, built initially in the early 1950's and extended in both 1962 and 1966, has a high average occupancy rate. An updated study with a different analysis also shows the Library to have an appreciable risk (Degenkolb and Associates, 1981). Based on these engineering studies, Campus Planning, Design, and Construction identified Rivera Library as the target structure for detailed analysis. It is the main campus library, with stacks for the humanities and social sciences, special collections, and a repository for government publications. Rivera Library was identified as the target structure because of its high occupancy rate and its scheduled seismic upgrade.

Because much of the city of Riverside sits on shallow sediments overlying basement rocks, ground motions are expected to be 7-10 times larger than those observed on basement sites (Envicom and County of Riverside, 1976). In the Seismic Safety Element for the County of Riverside, Envicom and the County of Riverside (1976) report that historic earthquakes in 1937, 1948, and 1954 on the San Andreas and San Jacinto faults were experienced in Riverside with "anomalously high intensities". This study did only a single assessment for the entire city of Riverside however, and a more focused study on the campus will refine (but not contradict) the analysis in the Seismic Safety Element (Envicom and County of Riverside, 1976).

1.4 Organization of this Report

This report presents results through December, 1998 with the installation of the seismic station at UCR. Potential seismic sources are reviewed, relying on efforts of SCEC scientists and UCR personnel to characterize these sources. New results of a detailed, broader study of the campus are also presented here. UCR personnel have expanded these efforts beyond the target structure in order to predict how ground motions might be affected at other locations on campus. Comparison of geophysical properties to mapped soil types will allow some prediction of these responses everywhere on campus.

Results from borings and logs are presented here. A new feature of this study is that all data are incorporated into a GIS data base for use by the campus. Topographic maps have been scanned and geographically registered. Borings from all past construction projects have been located and plotted. Building outlines from campus maps have been entered into the data base. Locations of all of our geophysical data and the new borings are in this data base.

Finally, recent earthquake records from the new UCR seismic station are shown.

2.0 SEISMOTECTONIC SETTING OF THE RIVERSIDE CAMPUS

2.1 Regional Setting

The UCR campus is located in the midst of the diffuse boundary between the Pacific and North American plates. While this western boundary of the North American plate is long-lived, it has only recently become a transform margin with one plate sliding past another. This transform margin has evolved in the past 28 My (Atwater, 1989), with the modern fault configuration in southern California developing in the past 5 My. The modern boundary is

characterized in southern California by blocks of crust sliding past one another and bounded by strike-slip faults (Figure 5). Total plate motion of 50 mm/yr is accommodated primarily by slip on the San Andreas fault (25 mm/yr), the San Jacinto fault (12 mm/yr), and the Elsinore fault (5 mm/yr) (Jackson et al., 1995). The remaining displacement occurs as deformation within blocks or on offshore faults. Two of these major faults, the San Andreas and San Jacinto, are within 30 km of the campus. Between the Salton Trough and the southern end of the San Joaquin Valley, the San Andreas fault has a major westward bend (Figure 5). Strike-slip faults are aligned parallel to the northwest relative plate motion north and south of this bend. Within this bend, there are components of motion both parallel and perpendicular to the San Andreas fault. The component of motion perpendicular to the fault leads to convergence of the crust within the east-west Transverse Ranges (Figure 5). This convergence is accommodated by uplift of the mountains and by thrust faulting along the southern boundary of the range. These thrusts are responsible for the significant seismic hazard in the Los Angeles basin, the Ventura-Santa Barbara region, and contribute to the hazard at UCR through the Cucamonga fault (Figure 6). While the largest historical earthquakes have been generated on strike-slip faults (Table 1; Figure 2), thrust faults in southern California have been responsible for several of the most costly recent earthquakes (1971 San Fernando and 1994 Northridge) and thus pose a hazard that cannot be ignored.

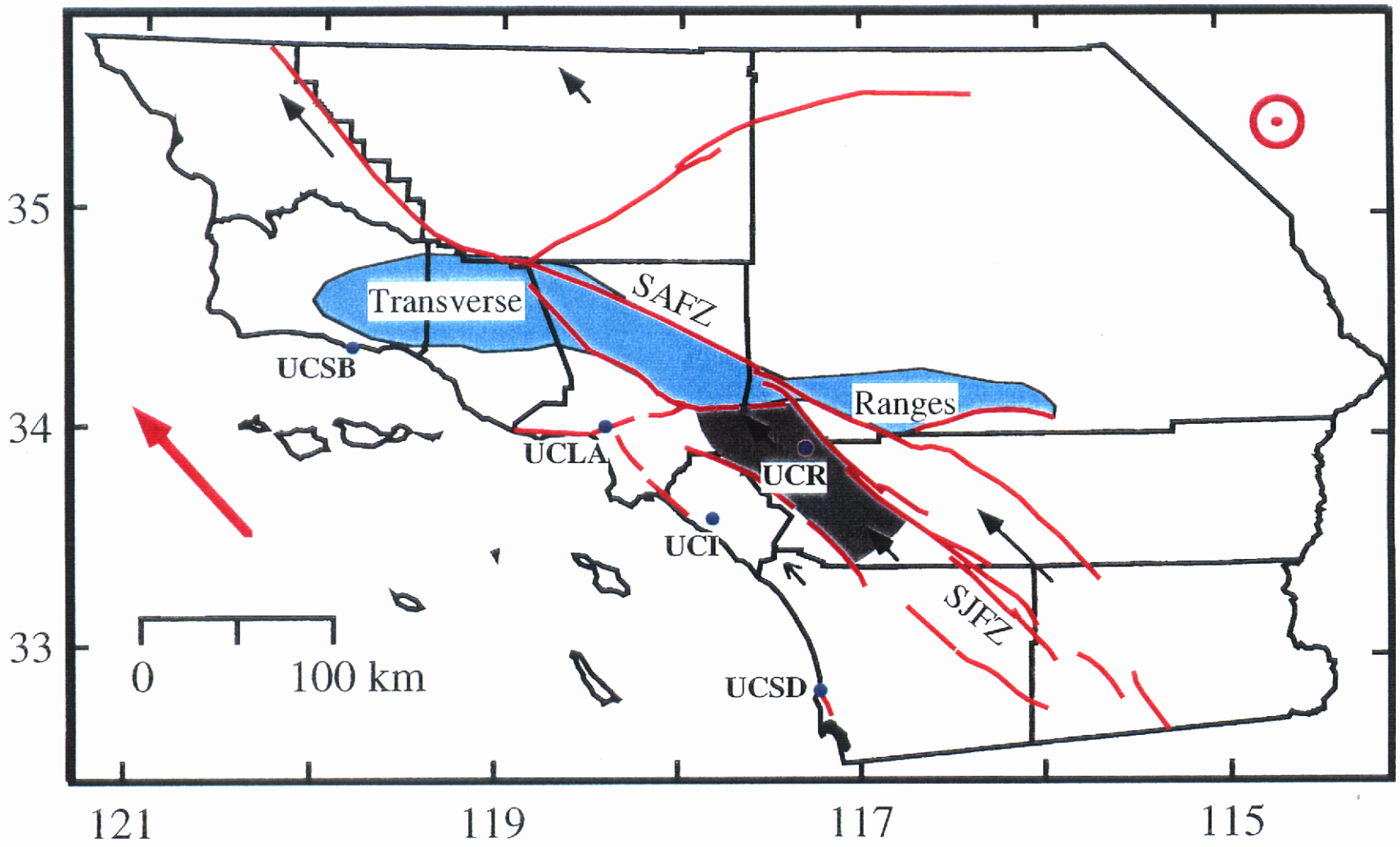

Figure 5 - Simplified tectonic map of southern California. Total motion of Pacific plate with respect to stationary North America is 4.8 cm/yr (magenta arrow). Block motions are scaled relative to this total motion. UCR sits on a segment of the southern California batholith identified as the Perris block (Woodford et al, 1971).

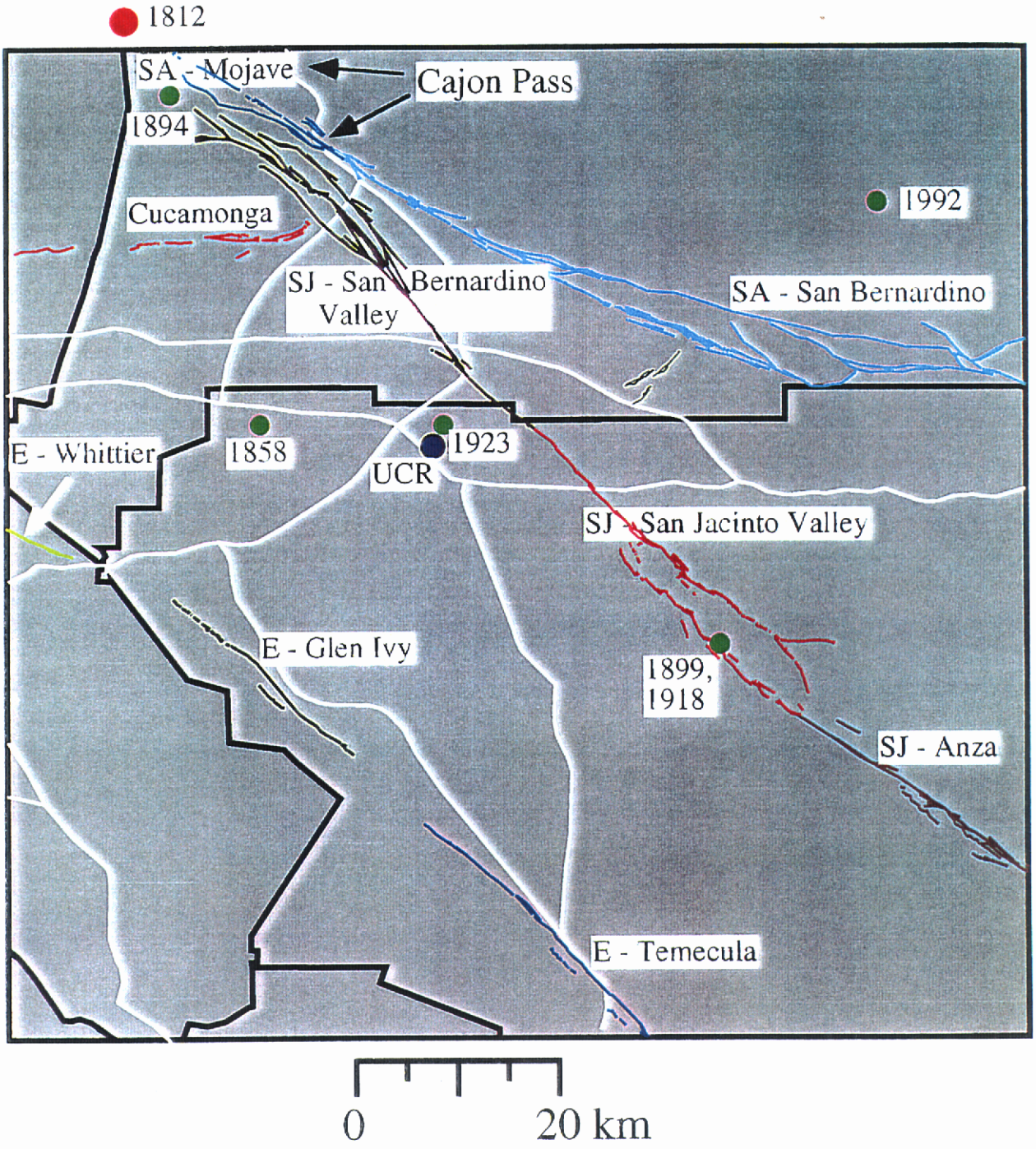

Figure 6 - Detailed fault map of inset region from Figure 1, showing segmentation of the Elsinore (E), San Jacinto (SJ), and San Andreas (SA) faults from Jackson et al. (1995). Earthquakes with magnitude Mw> 6.0 are shown. See caption of Figure 2 for explanation of symbols. Road network (white) and county lines (black) are also shown. Note that the locations of pre-1900 earthquakes are approximate. The southern terminus of the 1857 rupture zone is off the northwest corner of the map, near the town of Wrightwood.

Table 1 - Significant Earthquakes in southern California, 1769-1994. Ones that may have posed risk to Riverside are indicated in bold.

Year	Month	Day	Magnitude	Longitude	Latitude
1769	7	28	6.00	-118.000	34.000
1800	11	22	6.50	-117.300	33.000
1812	12	8	7.00	-117.650	34.367
1812	12	21	7.00	-119.900	34.200
1827	9	24	5.50	-119.000	34.000
1852	11	29	6.50	-115.000	32.500
1855	7	11	6.00	-118.100	34.100
1857	1	9	8.25	-120.300	35.700
1858[1]	**12**	**16**	**6.00**	**-117.500**	**34.000**
1862	5	27	6.00	-117.200	32.700
1872	5	3	5.75	-115.000	33.000
1875	11	15	6.25	-115.500	32.500
1883	9	5	6.25	-119.900	34.200
1890	2	9	6.50	-116.300	33.400
1892	2	24	7.00	-115.633	32.550
1892	5	28	6.50	-116.200	33.200
1893	5	19	5.75	-119.400	34.100
1894[1]	**7**	**30**	**6.00**	**-117.600**	**34.300**
1894	10	23	5.75	-116.800	32.800
1899[1]	**7**	**22**	**5.75**	**-117.600**	**34.300**
1899[1]	**12**	**25**	**6.40**	**-117.000**	**33.800**
1906	4	19	6.20	-115.500	32.900
1907[1]	**9**	**20**	**5.30**	**-117.100**	**34.200**
1910[1]	**5**	**15**	**5.50**	**-117.400**	**33.700**
1915	6	23	6.00	-115.500	32.800
1915	6	23	5.90	-115.500	32.800
1916	10	23	5.30	-118.900	34.900
1916	11	10	6.10	-116.000	35.500
1918[1]	**4**	**21**	**6.90**	**-117.000**	**33.800**
1923[1]	**7**	**23**	**6.00**	**-117.300**	**34.000**
1925	6	29	6.30	-119.800	34.300
1927	11	4	7.30	-120.800	34.700
1933	3	11	6.40	-117.967	33.617
1937	3	25	6.00	-116.267	33.400
1940	5	19	6.90	-115.500	32.733
1941	7	1	5.90	-119.583	34.367
1942	10	21	6.60	-116.083	33.050

Table 1 (cont.) - Significant Earthquakes in southern California, 1769-1994

Year	Month	Day	Magnitude	Longitude	Latitude
1946	3	15	6.00	-118.050	35.733
1947	4	10	6.50	-116.550	34.983
1948	12	4	6.00	-116.383	33.933
1949	5	2	5.90	-115.683	34.017
1951	12	26	5.90	-118.300	32.800
1952	7	21	7.50	-119.017	35.000
1952	7	21	6.40	-119.000	35.000
1952	7	23	6.10	-118.583	35.367
1952	7	29	6.10	-118.850	35.383
1952	11	22	6.00	-121.200	35.733
1954	1	12	5.90	-119.017	35.000
1954	3	19	6.40	-116.183	33.283
1968	4	9	6.50	-116.133	33.183
1971	2	9	6.60	-118.400	34.417
1973	2	21	5.20	-119.033	34.067
1979	10	15	6.40	-115.300	32.600
1981	4	26	6.00	-115.650	33.133
1981	9	4	5.90	-119.117	33.667
1986	7	8	6.00	-116.600	34.000
1987	10	1	5.80	-118.083	34.050
1987	11	24	6.20	-115.783	33.067
1987	11	24	6.60	-115.850	33.017
1992	4	23	6.10	-116.317	33.961
1992	6	28	7.30	-116.436	34.201
1992[1]	6	28	6.50	-116.827	34.202
1994	1	17	6.70	-118.533	34.200

[1]Earthquakes that appear on the local UCR map (Figure 6).
Data from Ellsworth (1990).

2.2 Earthquake Sources

Two faults contribute most of the seismic hazard to the UCR campus: the San Andreas fault and the San Jacinto fault. These are faults capable of generating peak ground accelerations in excess of 0.2 g. In addition, the nearby Elsinore and Cucamonga fault zones are capable of generating 0.1-0.2 g accelerations and will be included here. All of the discussion about seismic sources is taken from WGCEP (1988), Wesnousky (1986), Petersen and Wesnousky (1994), and Jackson et al. (1995). All of these references are compilations of results from original sources; see the compilations for the original studies. Most of the slip rates, probabilities, maximum magnitudes, and fault segmentation (Table 2) were taken from Jackson et al. (1995) as this is the most recent and comprehensive reference for seismic sources. Where calculated, moment magnitudes are determined from an empirical relation between segment length and the magnitude (Wesnousky, 1986). Estimates of ground accelerations are determined using an empirical relationship between acceleration, moment magnitude, and distance to the fault (Boore et al., 1993).

2.2.1 San Andreas fault: The San Andreas fault (SAF) is the most significant earthquake source in the vicinity of UCR and indeed in southern California. Of the three onshore fault systems south of the Transverse Ranges, this is the oldest with motions up to 5 My ago (Atwater, 1989). This fault is actually composed of four segments in southern California which sometimes rupture independently and sometimes together. The three southernmost segments, the Coachella, San Bernardino, and Mojave segments (Figure 6), are all capable of M_w>7.0 earthquakes (Jackson et al., 1995). Simultaneous rupture of the Mojave and Carrizo segments generated the 1857 M_w7.8 Fort Tejon earthquake, which was the largest historical earthquake in

Table 2 - Slip Rates, Recurrence Intervals, and 30-year Earthquake Probabilities[1]

Fault Segment	Slip Rate (mm/yr)	Maximum Magnitude	Last Rupture	Recurrence Interval (yr)	% Probability
San Andreas					
Mojave	30	7.5	1857	150(+123/- 71)	26±11
S. Bernardino	24	7.3	1812	146(+ 91/- 60)	28±13
Coachella	25	7.5	1690	160(+240/- 93)	22±12
San Jacinto					
S. Bernardino	12	6.7	1890	100(+150/- 50)	37±17
San Jacinto Valley	12	6.7	1918	83(+117/- 39)	43±18
Anza	12	7.3	1750	250(+321/-145)	17±12
Elsinore					
Whittier	2.5	6.9	650	760(+640/-274)	5±3
Glen Ivy	5	6.8	1910	310(+340/-146)	12±15
Temecula	5	6.8	1818	240(+260/-111)	16±10
Cucamonga	4	7.3	1971[2]	200[2]	-----

[1]Data from Jackson et al. (1995).
[2]See text for discussion of this fault and event.

southern California. The rupture of this earthquake terminated near the Cajon Pass in Wrightwood (Figure 6), and a repeat of this earthquake would likely result in rock accelerations at UCR exceeding 0.15 g. This is slightly larger than was experienced in 1992 as a result of the M_w7.3 Landers earthquake.

The Mojave segment of the SAF has paleoseismological evidence of at least 11 earthquakes since 529 A.D. (Sieh et al., 1989), resulting in an average recurrence interval (time between earthquakes) of 131 yr. However, the interval between events is extremely variable and both the WGCEP (1988) and Jackson et al. (1995) preferred a recurrence interval of 150 (+123, -71) yr based on the slip rate and estimated displacement in the 1857 earthquake. The unequal uncertainty on the recurrence interval results from the combination of uncertainties in slip and displacement. The conditional probability that the Mojave segment could rupture individually in the next 30 years is 26±11 % (Table 2).

The San Bernardino segment of the SAF is the least studied and the most structurally complex. Paleoseismological studies at Wrightwood reveal 6 events since 1192 A.D., leading to a recurrence interval of 133 yr (Biasi and Weldon, 1994). Jackson et al. (1995) preferred a recurrence interval of 146 yr based on slip rate and characteristic displacement. The most recent event appears to have been in 1812 in either case, with 186 yr elapsed since this earthquake. The conditional probability of an event on this segment in the next 30 years is 28±13 % (Table 2).

The Coachella segment of the SAF is the southernmost segment of the fault and reaches from the Salton Sea to San Gorgonio Pass. This segment has an average recurrence interval of 220 years based on paleoseismological data (Sieh, 1986) and has not experienced a large earthquake since 1680. Jackson et al. (1995) adopted this recurrence interval for their study. The

conditional probability for this segment is 22±12 % (Table 2).

Previous studies of seismic hazard have always treated these segments as individual sources (WGCEP, 1988; Wesnousky, 1986). Recent work on the San Andreas (Biasi and Weldon, 1994) has shown that these segments may be influenced by earthquakes on adjacent segments and occasionally rupture together. Accordingly, Jackson et al. (1995) allowed cascade events in which ruptures propagated across segment boundaries. This leads to a collective probability of 53% for at least one characteristic earthquake on the southern San Andreas in the next 30 years (Jackson et al., 1995).

2.2.2 San Jacinto fault: The San Jacinto fault is relatively young, with a total offset of only 28 km and motion beginning no earlier than 2.5 My ago and more likely 1.5 My ago (Morton and Matti, 1993). This fault is divided into 7 segments, but only the northernmost three (San Bernardino, San Jacinto, and Anza) contribute to the seismic hazard at UCR (Figure 6). While these segments cannot generate earthquakes as large as those on San Andreas fault, they are much closer to UCR (8.5 km) and thus capable of comparable ground motions. If the San Jacinto and San Bernardino segments rupture together (Park et al., 1995), then the combined earthquake could be large (M_w 7.5). Alternatively, Sanders and Magistrale (1997) have subdivided this fault into many, smaller segments, which could lower the maximum magnitude for any one segment. This latter work has not been incorporated into hazard models yet, so this discussion will focus on the accepted segmentation model. Current paleoseismological studies of the San Bernardino segment reveal low slip rates, but slip values of 12 mm/yr are preferred because there is no record of multiple earthquakes (Jackson et al., 1995). This higher slip rate is based on more extensive paleoseismological studies on the Anza segment and the lack of

structures across which slip can be transferred. The 1890 M_w=6.5 earthquake occurred on this segment, and the 1899 M_w=6.4 earthquake may have also ruptured this segment. Both of the earthquakes likely produced ground accelerations exceeding 0.2 g at the location of the UCR campus. The conditional probability of a rupture on the San Bernardino segment of the San Jacinto fault is 37±17 % (Jackson et al., 1995). The location of the 1923 M_w=6.0 earthquake that occurred just north of the campus (Figure 6) is uncertain to within 10 km and likely occurred on the San Bernardino Valley segment of the San Jacinto fault.

The San Jacinto Valley segment is located just east of Moreno Valley, spanning from the Box Springs Mountains to Hemet, and was the source of the 1918 M_w=6.8 earthquake (Figure 6). It has a recurrence interval of 83 yr and a conditional 30-yr probability of 43±18 % (Jackson et al., 1995). The Anza segment (Figure 6) extends to the southeast of Hemet and last experienced a moderate earthquake in 1750 (Rockwell et al., 1990). It has a recurrence interval of 250 yr and a conditional 30-yr probability of 17±12 % (Jackson et al., 1995). If possible interactions between segments are allowed, then the conditional probability of at least one characteristic earthquake occurring on the San Jacinto fault in the next 30 years is 72% (Jackson et al., 1995). Earthquakes on either of the San Bernardino or San Jacinto segments, whether cascaded ruptures or ruptures on single segments, are capable of generating horizontal accelerations exceeding 0.3 g at the UCR campus.

2.2.3 Elsinore fault: The Elsinore fault is the youngest of the three major onshore strike-slip faults accommodating the transform motion, with a total offset of 5-11 km (Powell, 1993) and estimated maximum ages of 2.5 Ma based on total offset and modern slip rate. It also has the least slip - 4-5 mm/yr (Jackson et al., 1995). The northern portion of the fault zone is

divided into the Whittier, Glen Ivy, and Temecula segments (Figure 6). One of the difficulties with paleoseismological studies of this fault is that only two earthquakes in the past 100 years have produced surface ruptures (Jackson et al., 1995). Studies of fault offsets from individual events will then result in an incomplete record and underestimate the seismic hazard. Recurrence intervals are estimated from average slip rates and estimates of average offset per earthquake. The latter value can be determined from paleoseismological records of infrequent breaks on some segments and empirical relations between segment length, moment magnitude, and offset per earthquake (Wesnousky, 1986). Both methods were used on segments of the Elsinore fault because of lack of historic and Quaternary earthquakes.

The northernmost Whittier segment has a slip rate approximately half of the other segments because some of the motion is transferred to other faults where the Elsinore fault enters the Los Angeles basin (Jackson et al., 1995). Paleoseismological evidence of earthquakes is sparse, with only two events recorded (Rockwell et al., 1992). The most recent of these events was 1400-2200 yr ago. A recurrence interval of 760 yr is calculated from the slip rate of 2.5 mm/yr and the amount of slip in this event (1.9 m) by Jackson et al. (1995). A conditional 30-yr probability of only 5±3 % is determined for this segment.

The Glen Ivy segment has a higher slip rate (5 mm/yr) and paleoseismological evidence of at least five earthquakes since 1060 A.D. (Rockwell et al., 1986). Jackson et al. (1995) estimate a recurrence interval of 310 years and a conditional probability of 12±15 % for this segment. The 1910 Temescal Valley earthquake ($M_w \approx 6$) was the only historic earthquake on this segment. The Temecula segment also has a higher slip rate (5 mm/yr) but no paleoseismological evidence of earthquakes (Jackson et al., 1995). A recurrence interval of 240 years is based on slip and

estimated maximum displacement per event, and a conditional probability of 16±10 % is calculated for this segment (Jackson et al., 1995).

Simultaneous rupture of adjacent segments is permitted for this fault also, and there is a 21% probability that at least one characteristic earthquake will occur on this fault in the next 30 years (Jackson et al., 1995). If the Glen Ivy and Temecula segments rupture together, then this fault is capable of producing a M_w=7.0 earthquake.

2.2.4 Cucamonga fault: This east-west striking thrust fault forms the southern boundary of the Transverse Ranges just west of Cajon Pass (Figure 6) and accommodates convergence across the bend in the San Andreas fault. Jackson et al. (1995) treat the Cucamonga fault zone as the eastern extension of the Sierra Madre fault which extends for approximately 85 km along the southern edge of the Transverse Ranges. This fault produced the 1971 San Fernando earthquake (M_w=6.7). Slip rates of 4 mm/yr are determined only for the Cucamonga fault (Morton and Matti, 1987), but extrapolated along the entire Sierra Madre fault by Jackson et al. (1995). Paleoseismological studies indicate recurrence intervals of 200 years for events similar to the San Fernando earthquake. In contrast, Wesnousky (1986) used a recurrence interval of 700 years for the Cucamonga fault itself.

3.0 UCR SOURCE AND SITE CHARACTERIZATION

3.1 Geological Setting for the UCR Campus

The UCR campus lies on a stable block (the Perris block) of the southern California batholith bounded by the Cucamonga fault to the north, the Elsinore fault to the southwest, and

the San Jacinto fault to the northeast (Figure 5). The batholith was formed from magma generated along the western margin of North America as a result of subduction of the Farallon plate and is older than 80 Ma (Todd et al., 1989). The Perris block shows little to no internal deformation and is converging northward towards the Transverse Ranges (Woodford et al., 1971). Beginning 50 Ma ago, the surface of the block has experienced several phases of erosion and deposition of continental sediments (Woodford et al., 1971). Based on the positions of these erosional surfaces, Woodford et al. (1971) infer that the block has experienced vertical motions of a few hundred meters, but no tilting. In general, deformation (and thus earthquake activity) is confined to the perimeter of the block.

The composition of the batholithic rocks ranges from granitic to tonalitic, but locally are quartz diorite and quartz monzonite (Menzie, 1962). Outcrops of crystalline rocks are seen in the surrounding Box Springs Mountains and on the campus itself (Figure 7). The overlying alluvium consists of weathered granitic rocks with abundant angular fragments of feldspar, quartz, and biotite. The alluvium is poorly sorted, has indistinct layering, and has grain sizes generally ranging from gravel to clay-sized particles. In borings on the campus, this unit is invariably described as brown sand (Elrick, 1998).

The campus is located on alluvium in a bowl-shaped depression against the Box Springs Mountains. This bowl has resulted from erosion of the mountains, and active channels still cross the campus. Several borings (Figure 8) have penetrated bedrock, although most have not. Bedrock was penetrated at a depth of 88 m next to Rivera Library, a depth which is consistent with nearby water wells and borings that indicate depths of less than 100 m. A much more extensive study of bedrock to the east beneath March ARB (Lee et al., 1997; Zawila, 1997) has

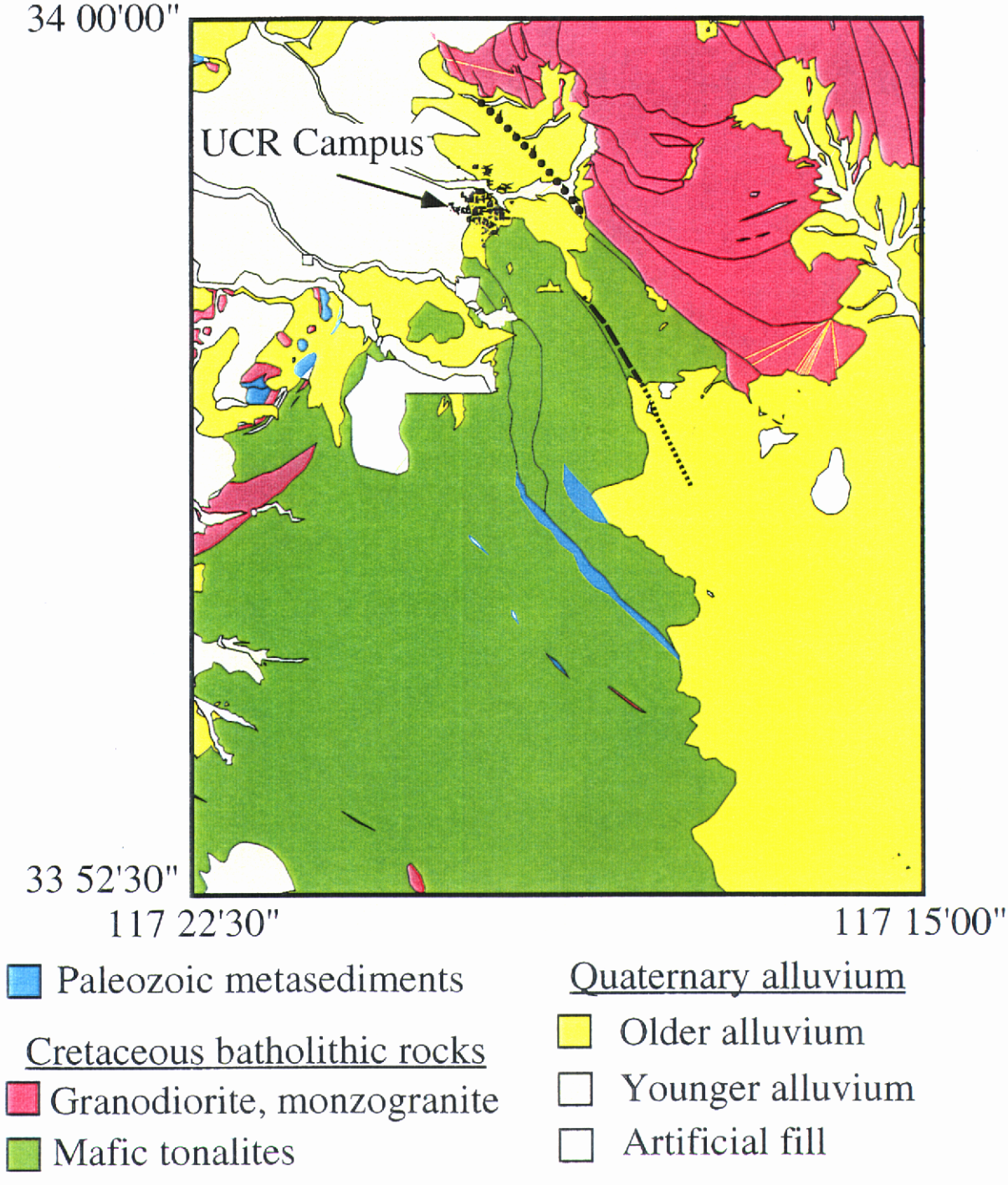

Figure 7 - Simplified geologic map of the region around the UCR campus (adapted from Morton and Cox, 1988). Solid/dashed line is unnamed fault from Morton and Cox, while dotted line is the Box Springs fault from Menzie (1962). Both are inactive.

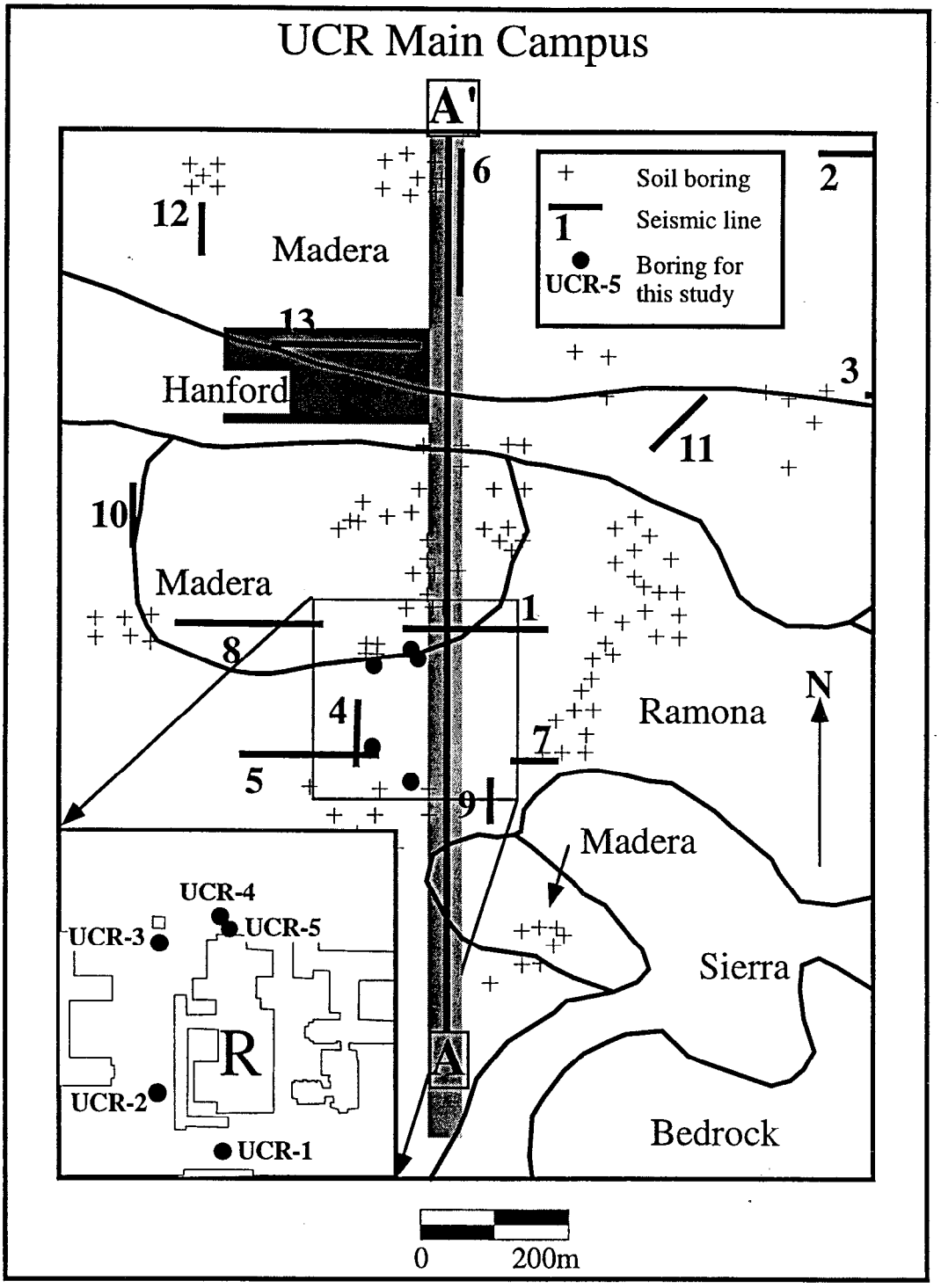

Figure 8 - Locations of seismic lines and soil borings used in the database. UCR-1 to UCR-4 are Cone Penetration Test sites (no samples). UCR-5 is the deep hole wherefrom soil samples were taken (see inset). A geologic cross-section along AA' was constructed from all data, and is presented in Figure 10. The Intramural (IM) field is the dark grey rectangle, and gravity profile is denoted by the light grey box along AA'. Soil unit names are shown, along with contacts. The modern drainage generally follows the distribution of the Hanford soil on campus. R" in inset denotes the Rivera Library.

shown that bedrock depths in alluvial settings can be extremely variable. Bedrock patterns in very shallow areas appear to follow modern drainages, however. If so, then alluvial thicknesses are likely greatest in the region of the intramural (IM) field and between the dormitories (Fig. 8). The main part of the campus is underlain by three soil units (Figure 9). Two of these, the Ramona loam and the Madera sandy loam, are older soils while the Hanford sandy loam is younger (Nelson et al., 1917). Loams contain contain 25-50% sand, 0-25% clay, and 25-50% silt, while sandy loams contain 50-80% sand, 0-20% clay, and 5-50% silt. In general, sandy loams are coarser grained than loams. In studies of comparable soils in the Los Angeles basin, Tinsley and Fumal (1985) assigned Pleistocene ages to the Ramona and Madera soils and Holocene ages to the Hanford soils. The Madera sandy loam is brown-reddish brown, medium-grained, and friable to a depth of 30-40 cm but develops a hardpan in the B horizon at depths of 1-1.5 m that must be blasted for root penetration. Below the hardpan, this soil is friable. This loam is low in organic matter and derived from erosion of granitic rocks (Nelson et al., 1917). The Ramona loam is also a brown, gritty, and friable soil ranging from 30-45 cm thick at the surface. Its texture is relatively uniform to depths of 2 m or more and generally does not develop a hardpan. It is also derived from granitic rocks and is a compact soil (Nelson et al., 1917). Gravel is commonly present in the section. Well-developed subsoils exist for both of these older units.

The Hanford sandy loam is brown, friable, and smooth-textured to depths of 2 m or more. Seams of sand and gravel are present. Based on the ease of tilling and drainage reported by Nelson et al. (1917) for this soil, we infer that it is less indurated than the older soils. This soil is also derived from erosion of granitic rocks (Nelson et al., 1917). In some areas, this soil is found

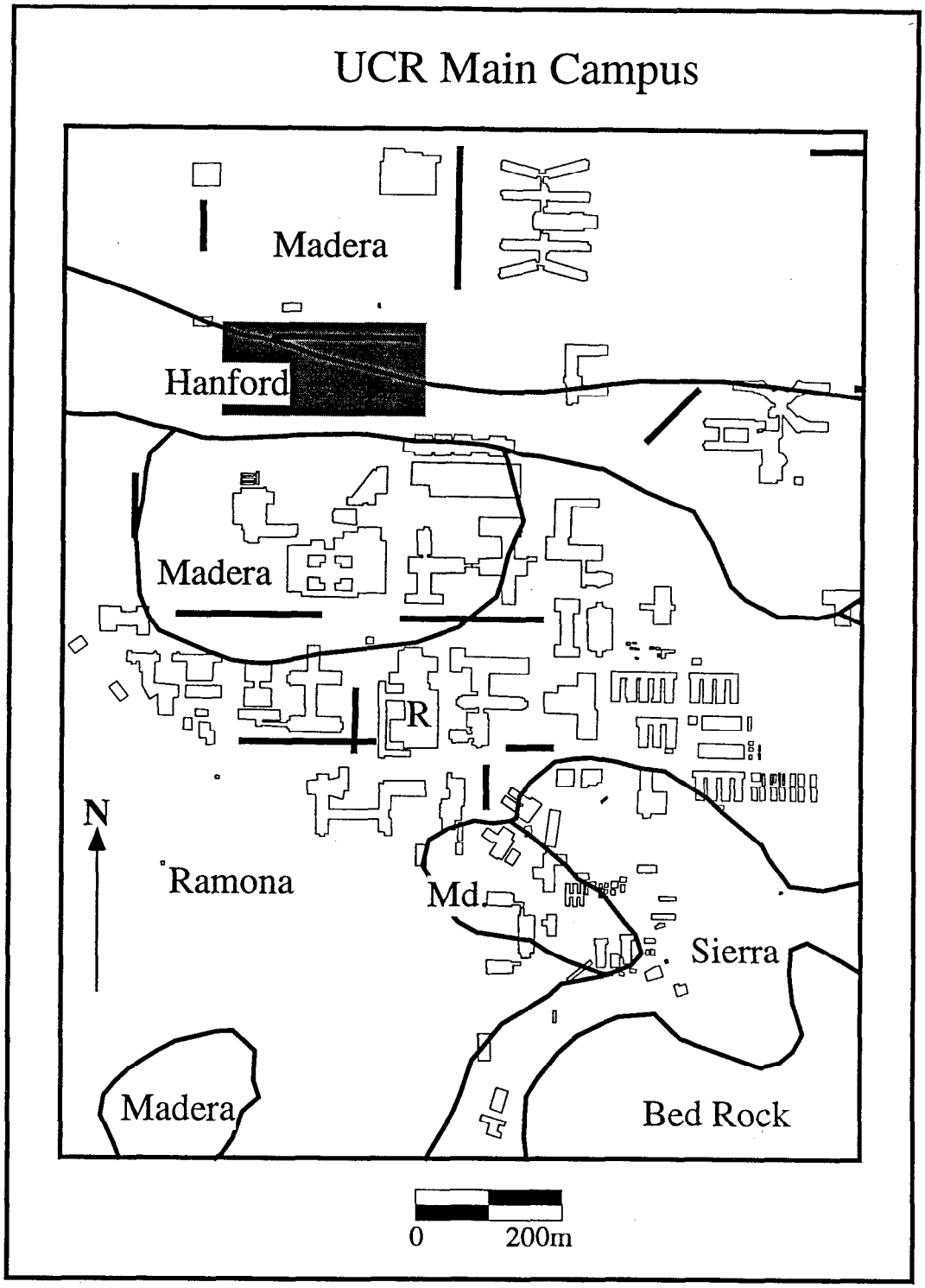

Figure 9 - Map of UCR buildings with soil units, seismic lines, and IM field (dark grey box) from Figure 8. Soil units are taken from Nelson et al. (1917). See captions of Figure 4 and 8 for explanation of symbols.

in recent or active drainages. However, active drainages are also found crossing the older soils.

The Sierra loam occupies the southeastern corner of the campus (Figure 9) and is found mainly on the bedrock slopes. In many areas, this soil is very thin; granitic outcrops are found within this unit, for example. It grades into weathered granite at its base (Nelson et al., 1917). Given its restricted distribution, relative thinness, and underlying bedrock, we did not focus any effort on this unit.

More recent maps of the Quaternary surficial units group both the Madera and Ramona units into a single Pleistocene compact, dense, medium-grained unit found on inactive alluvial fans and plains and overlying bedrock (Tinsley and Fumal, 1985). The Hanford unit is identified as a younger (Holocene) medium-grained unit in active alluvial fans which overlie Pleistocene alluvium. The Hanford unit is generally less than 10-m thick in the inland basins (Tinsley and Fumal, 1985). We have elected to keep the Ramona and Madera units separate for our study because we will show that there are significant differences in the geophysical properties of each.

There are very few mapped faults within close proximity to the UCR campus (Figure 7). The closest recognizable fault is located east of campus near Moreno Valley, but it is inactive (Doug Morton, personal communication, 1998). Less than a mile east of campus, the informally named Box Springs fault was mapped by Menzie (1962) and Joshi (1967). However, the fault was mapped as concealed at that time and more recent detailed work (Morton and Cox, 1988) shows no evidence of this fault either to the southeast of the campus in bedrock or to the north in bedrock. Students in a field geophysics course at UCR have mapped an offset in bedrock on Big Springs Road to the east of Watkins Drive (Figure 7), but the offset appears to be too flat to be a fault. More likely, it is an expression of the foliation in the granitic rocks (Morton, personal

communication, 1998). In any case, there has been no earthquake activity on this structure and it is likely inactive.

3.2 Compilation of Foundation Borehole Data at the UCR Campus

Records from 104 borings were compiled into a data base for use on this project. The borings consisted of soil logs (and geotechnical measurements in some cases) made for structural studies prior to construction of the existing buildings. The distribution of borings was extremely uneven (Figure 8), reflecting primarily the construction of the newer buildings. In addition, the soil descriptions were very uneven. Some contractors used the Unified Soil Classification System (USCS), while others did not. We have attempted to standardize the data base by using the USCS throughout, but had to interpret the nonstandard descriptions. Nonetheless, a cross section of the campus was constructed from the borings in close proximity to profile AA' (Figure 8). This profile (Figure 10) shows a relatively uniform layer of brown, silty sand overlying brown sand in both the Ramona and Madera soils. Bedrock is penetrated at the southern end of the profile in one boring at a depth of 6 m. The Hanford sandy loam shows up clearly as a thin (3 m thick) layer of brown silty, clayey sand overlying an older soil horizon inferred from the orange color (indicative of weathering) and roots (Figure 10). The Hanford soil is very restricted both areally and in depth. Thus, much of the focus of the seismic study at UCR was on the Madera and Ramona units.

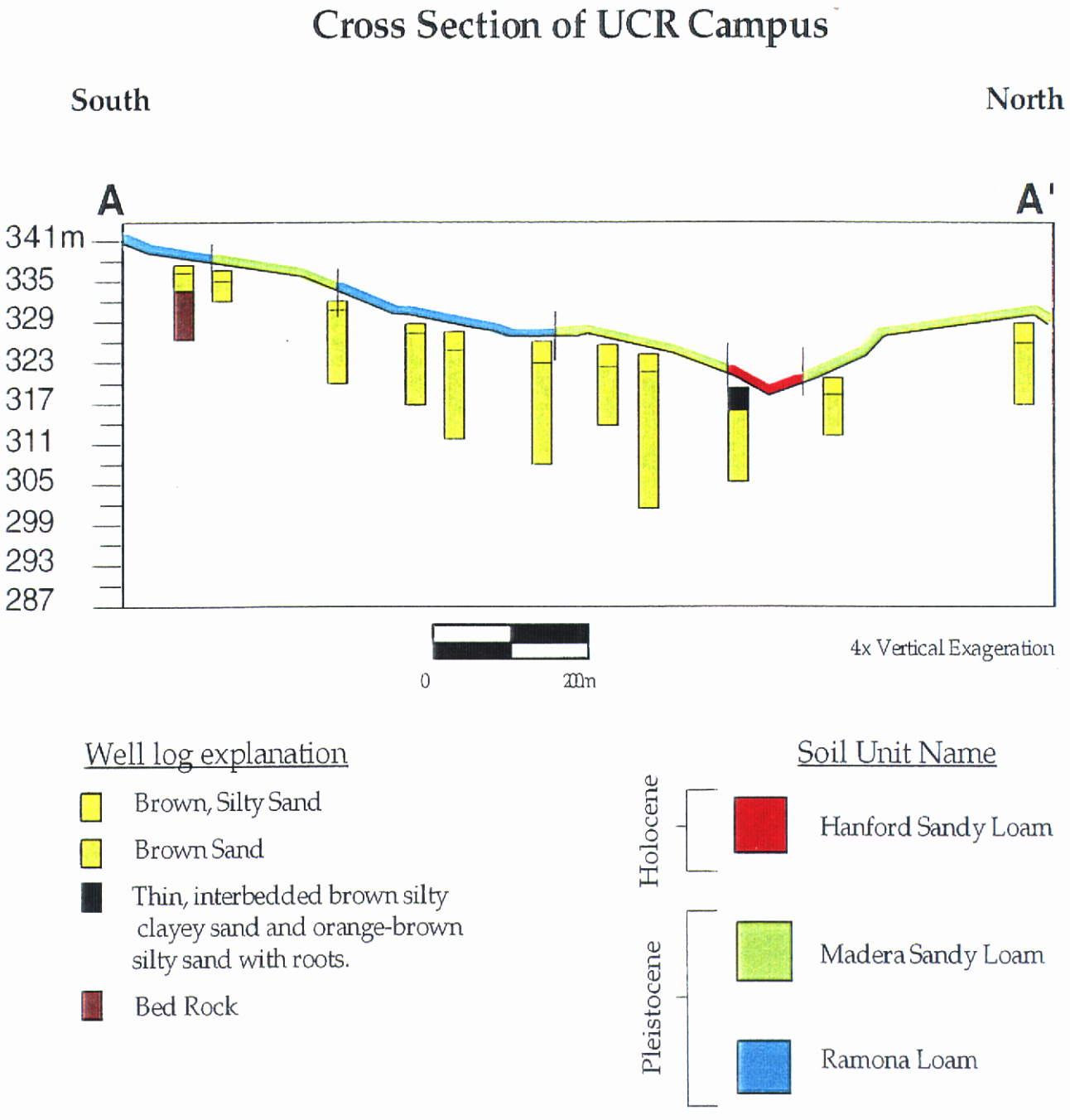

Figure 10 - Cross-section of UCR campus along AA'. The description of sediments encountered in borings is taken from the records. Soil units are assigned at the surface and are from Nelson et al. (1917). Note the thinness of the Hanford sandy loam.

3.3 Gravity Profiling at the UCR Campus

We collected a profile of 30 gravity stations spanning the campus from south to north which overlapped partially with profile AA' (Figure 8). This gravity profile extended from bedrock exposures at the southern edge of campus to outcrops off campus to the north. These gravity measurements were processed with standard analysis techniques and reduced to a simple Bouguer anomaly (Telford et al., 1990). Topography in the vicinity of the stations was very gentle (the profile in Figure 11 has a 5:1 exaggeration) except at the ends of the profile, so terrain corrections are likely small. The gravity profile confirms that the campus sits in the southern half of a shallow basin (Figure 11) with a maximum gravity signature of 3 milligals. Two-dimensional computer modeling (Malinconico and Larson, 1989) was used to develop a subsurface basin profile which was consistent with both the deep and shallow borings on campus. Gravity interpretation is non-unique, and multiple models can often fit the same observed data. External constraints from borings and geophysical logs play a key role in limiting the range of possible models. Soil densities from the upper 21 m are consistently in the range of 1900 kg/m^3. Basement densities (Morton, personal communication, 1998) are 2770 kg/m^3 in this area, leading to a density constrast in the upper 21 m of approximately -900 kg/m^3. Based on the geophysical logs in the CLC deep borehole, we established a two-layer model with this larger density constrast at depths shallower than 30 m and a lesser constrast between depths of 30 m and 88 m (basement). Then, we adjusted this lesser density contrast until the predicted gravity anomaly fit the observed data at the borehole. Basement depths to the south of the deep borehole from profile AA' were also used as constraints (Figure 10). Once this deeper density contrast was constrained, the shape of the basin to the north was varied until the gravity profile

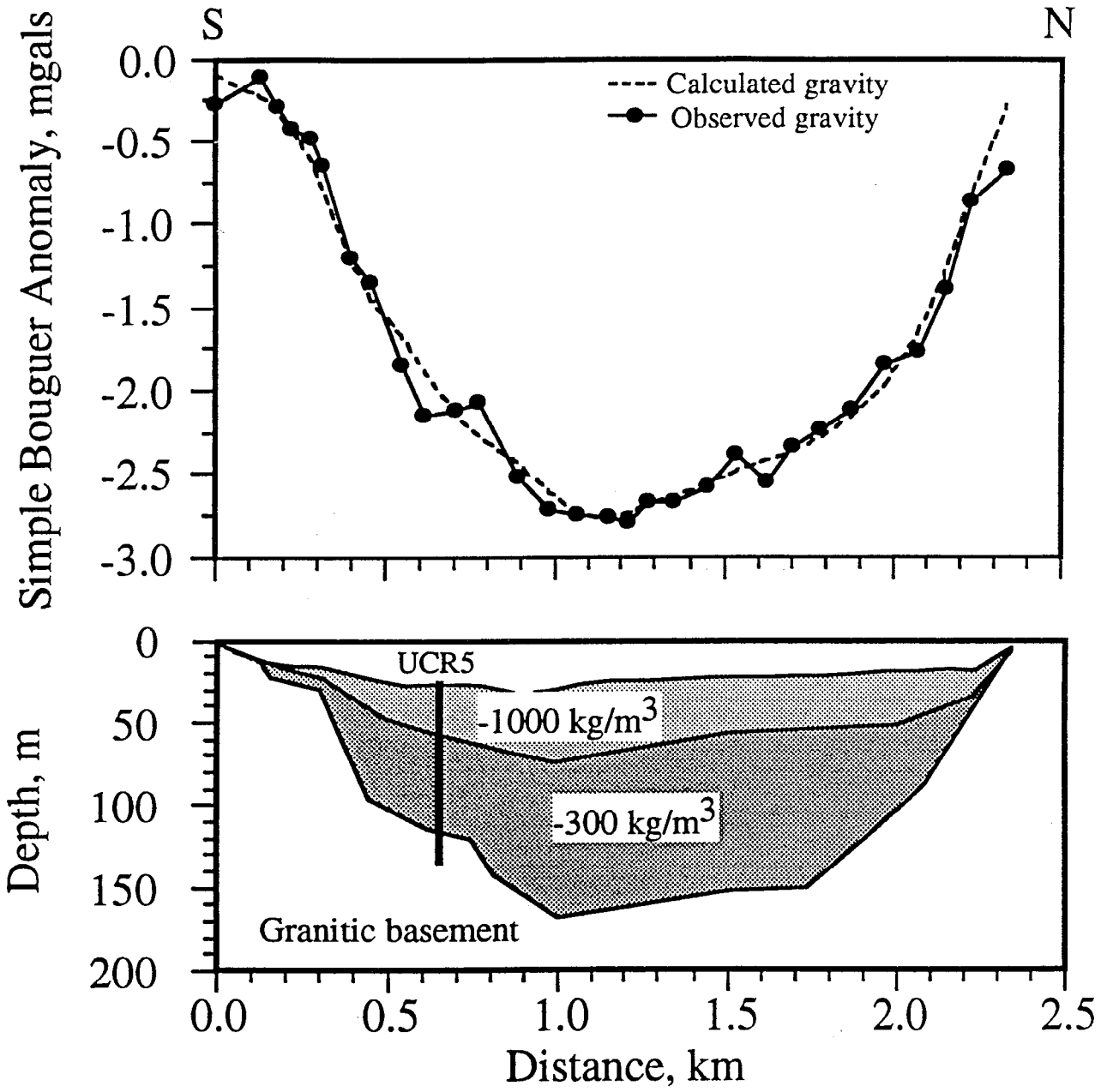

Figure 11 - Density model of the gravity profile across the UCR campus. The vertical black line in the cross-section is the deep borehole (UCR-5) for the seismic station. Density contrasts are computed with respect to the granitic basement. The granitic profile is tied to granitic outcrops at the northern and southern ends of lines.

was fit (Figure 11).

The final density contrast used in the upper 30 m at the deep borehole was -1000 kg/m^3; we were unable to fit the depth and gravity constraints with the initial contrast from the soil and basement densities. A density contrast of -300 kg/m^3 between the deeper sediments and basement was found to jointly match the depth constraints from the borehole and the observed gravity anomaly. With these constrained density contrasts, the sediment thickness in the deepest part of the basin is estimated to be 130-150 m. There may be considerable uncertainty in this depth because much of the gravity anomaly is controlled by the thickness of the shallower, less dense soil (Figure 11). We have assumed that its thickness does not increase dramatically from its value at the deep borehole. If this unit increases to 60-m thick, the gravity anomaly can be explained entirely with the shallow sediment layer. Indeed, our pre-drilling estimates of depth to basement were based on this single layer model. The constraints from the borehole now require that the thicker, deeper sediment layer be present. In summary, sediment thicknesses elsewhere on campus may be as little as 60 m and as great as 150 m. The latter bound is preferable because it extrapolates a layer known to be in the deep borehole beneath the entire campus, albeit with variable thickness.

3.4 Shallow Seismic Refraction Surveys at the UCR Campus

Studies of ground motion have shown that seismic waves are dramatically altered in the uppermost 30 m (Anderson et al., 1996) and that there is an empirical correlation between the local amplification factor and the average horizontal shear (SH) wave velocity in the uppermost 30 m (Borcherdt, 1994). Higher shear-wave velocities are indicative of more indurated sediments

which will shake with lower levels of acceleration. The basic problem is that any measurement of SH wave velocity is areally restricted because it is measured in a borehole or with a short (200 m) seismic line. A common practice is to use the surface geology to extrapolate the SH wave velocities beyond the measurement point (Fumal and Tinsley, 1985; Park and Elrick, 1998). Sufficient numbers of measurements must be taken in each geologic unit in order to adequately characterize that unit. With this philosophy in mind, we designed the seismic survey of the UCR campus to sample all three major soil units. A complete description of this study is given in Elrick (1998).

While we are interested primarily in shear-wave velocities, both P (compressional) and SH waves were measured because interpretation of shear-wave records can be problematic. If a common geometric structure can be found to fit both P and SH arrivals (but with different velocities), then there is greater confidence in the resulting structure. Lines were sited in locations where the surface was planar (although not necessarily horizontal) and a minimum of underground structures such as utility conduits, pipes, and tunnels crossed the line. Lines were located on lawns or in dirt because the geophones had to be buried. As much as possible, lines were confined to the central portion of the campus where most of the existing and planned buildings are concentrated. A total of 13 lines were sited, with 6 each on the Ramona and Madera soils and one on the Hanford soil (Figures 8,9). Only one line was sited on the Hanford soil because of access to this unit. While the Hanford unit is shown on the southern half of the IM field, this field was built on a cut-and-fill structure where the Hanford soil was probably removed. The cross section through campus shows that the Hanford soil is less than 3 m thick at the east end of the IM field (Figure 9).

Nominally, a line length of at least 150 m would be needed to penetrate 30 m. A line length of 200 m was used whenever possible, but logistical considerations limited this to 100 m or less at several of the lines (Figure 9). Each line consisted of 24 geophones spaced 4 m apart. Shotpoints were placed at a distance of 1-4 m from the first and last geophones, making a line 100 m long from shot to shot. At the 200-m lines, additional shot points were placed 50 m from the first and last geophones. Geophones were planted in 15-30 cm deep holes dug through the ground cover. This depth permitted us to plant the phones below the root mass for the vegetation. Both P and horizontal S phones were placed in the same hole with the axes of the S phones aligned transverse to the seismic line. All S phones were aligned so that they had the same polarity. They were then covered to prevent any wind noise.

Two seismic sources were used for the refraction surveys. The first was an SH source described by Pearson (1994). This unit used compressed gas to fire two 45-kg weights against stops, thereby imparting an impulsive horizontal ground motion (Figure 12). This source was held firmly to the ground by parking the front end of a heavy truck on it. The source was operated on both dirt and concrete initially, but better data resulted when it was on the dirt. The SH source was aligned transverse to the seismic line and thus parallel to the SH geophones. The second source was used to generate P waves and consisted of a 7.2 kg sledgehammer and a metal plate. This latter source was emplaced by digging through the root mass at the surface and placing the metal plate on the dirt below. Then, the plate was struck several times in order to seat it in the soil. Despite these preparations, the P source was incapable of generating observable first arrivals beyond 100 m. The SH source was clearly visible at distances of up to 200 m, however.

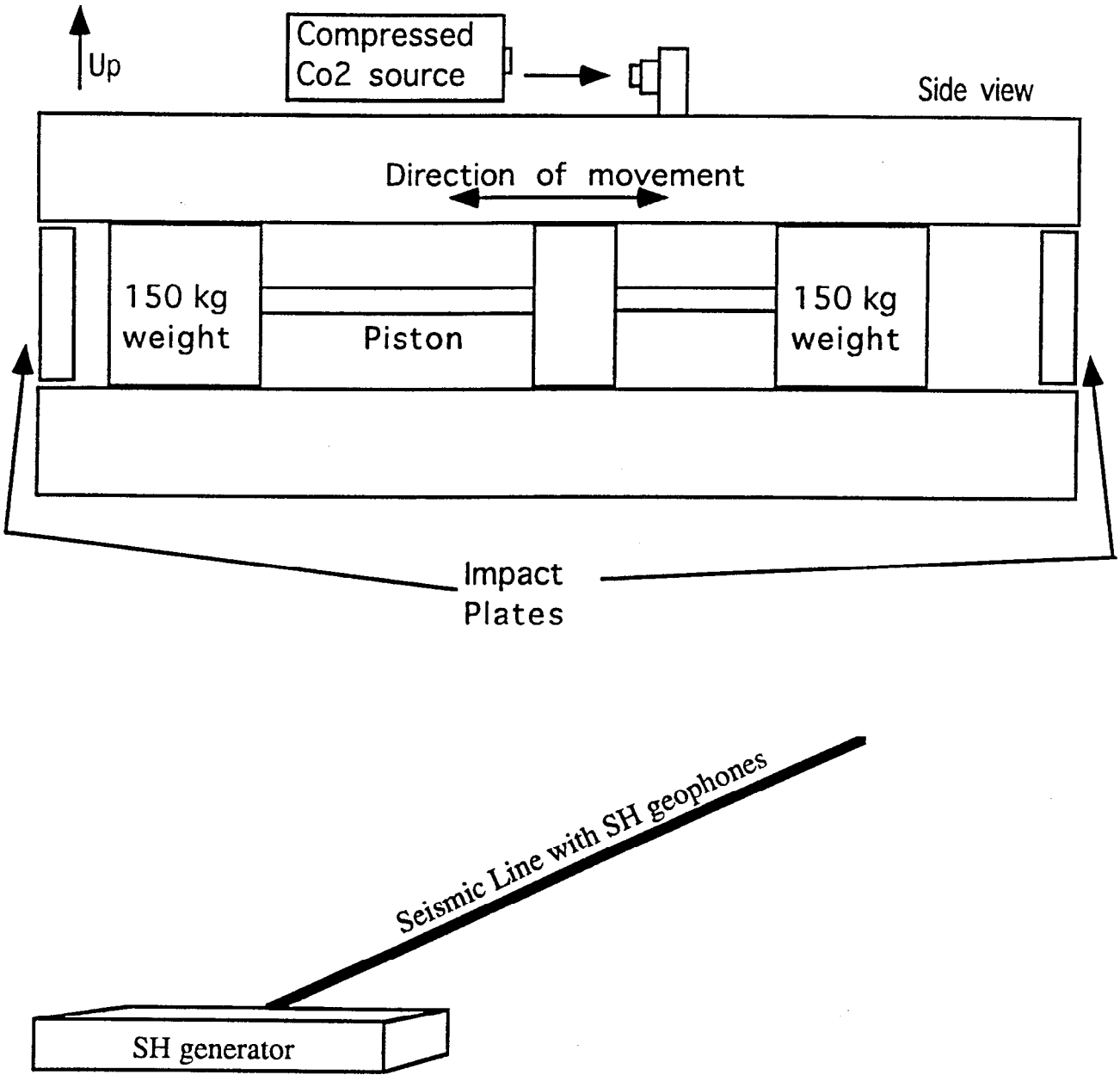

Figure 12 - Schematic of the shear-wave generator and its alignment with respect to the seismic line. The generator produces SH waves, with ground motion perpendicular to the line and parallel to the earth's surface.

Data were recorded digitally on a Geometrics Strataview 24 bit seismic recorder. The recorder was triggered by a geophone (P or SH) placed within 3 cm of the P or SH source. A total of 8192 points in a record 1024 msec long were recorded for each channel, yielding a sample rate of 0.125 msec per point. No filtering was used, except for a 250 Hz high cut filter and a 180 Hz notch filter. A notch filter at 60 Hz was tried, but it attenuated the seismic arrivals also (Figure 13). One advantage of digital recording was that multiple shots could be stacked in order to improve the signal-to-noise (S/N) ratio. A minimum of 16 repeated shots were stacked for each SH source location, and 32 stacks were used for the shot points located 50 m from the ends of the lines. Different numbers of repeated shots were used with the P source, but we found that there was no difference in the record quality with more than 8 stacks. Thus, P sources were stacked 8 times for each shot.

The SH source was capable of generating a polarized signal, depending on whether the weights were fired to the left or to the right. Thus, we obtained records with both polarities and used the polarizable nature of the signal to differentiate between SH and other arrivals. Because the velocity of the shear wave in the soil typically ranges from 200-600 m/s, it is possible to confuse the SH first arrivals with the arrival of the ground roll (a surface wave) or the air wave traveling at the speed of sound in air (330 m/s). We may also get SH-P wave conversions off of nearby structures which are parallel to the seismic line. Most of these other waves will have the same polarity, regardless of which way the SH source is fired. For example, the air wave is a sound wave resulting from the impact of the weights against the stops and is always a compressional wave traveling outward from the source. The polarity of its arrival at the geophone (i.e., which way the geophone moves first) is the same whether the SH source is fired

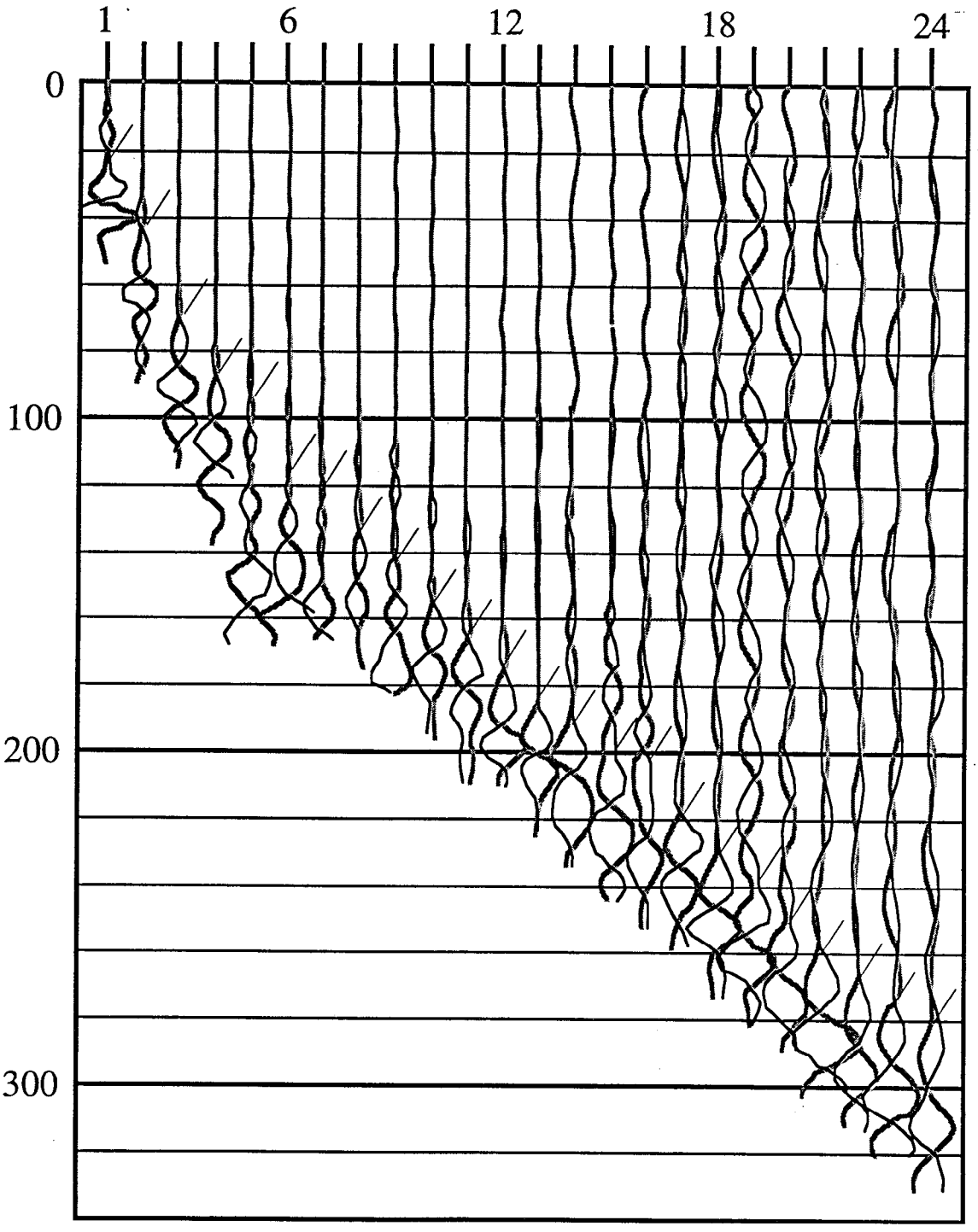

Figure 13 - Sample seismic record for shear-wave study. Two records with opposite source polarity are overlaid in order to identify shear-wave arrivals (thin lines) at each of 24 geophones. Travel times in milliseconds (vertical scale) and associated uncertainties are recorded for each geophone.

to the right or to the left. By collecting records of first arrivals with both polarities from the SH source, we can overlay the two and clearly identify the SH arrival (Figure 13).

First arrivals were picked from the digital records using the analysis software SIPC from RimRock Geophysics (1995). First arrivals and quality factors based on the uncertainties in the arrival times were stored in files and used in the interpretive phase of the study. Uncertainties in arrival times increased with shot-receiver distance. For shorter distances (less than 100 m), uncertainties were typically less than 5 msec. At longer distances (150-200 m), uncertainties were typically 10 msec. Larger uncertainties were assigned to particularly noisy geophones or unclear arrivals. In a few cases, arrivals were not clear at all and the first arrival could not be picked.

Data were interpreted using both forward and inverse models. The inverse model represented the structure with layers of constant velocity separated by irregular interfaces (Rimrock Geophysics, 1995). The forward model, MacRay, uses 2-D ray tracing though a model that permits both horizontal and vertical velocity gradients within layers separated by irregular interfaces (Luetgert, 1992). Because velocity gradients are often found in shallow environments, the forward model was preferable for the final interpretation. The inverse program was therefore used to provide an initial model for the forward program. This initial model was then refined with trial-and-error iterative fitting of the data. Because the P and SH arrivals are modeled separately by this program, we took special efforts to ensure that structural discontinuities (interfaces between layers) were common to both models. The P and SH lines were fit with structures which were consistent with each other.

An example of the interpretation for line 11 is shown in Figures 14 and 15. The arrival times for the P waves were fit to within the uncertainties of the data (Figure 14) by a layered structure with vertical velocity gradients within each layer. Rays penetrated to depths of 32 m, where velocities of approximately 900 m/s were encountered. A 3-m thick layer with large vertical velocity contrasts (200 m/s-400 m/s over 3 m) was needed to fit the data (Figure 14). Structure in the S-wave velocity model was similar, with a layer boundary at 3 m and minimal lateral velocity gradients in this upper layer (Figure 15). This model also fit the data to within uncertainties of the SH-wave arrivals. Rays penetrated to depths of 40 m in the S-wave model, where velocities of 760 m/s were encountered (Figure 15). Near the upper surface of the lower layer, horizontal velocity gradients of 1.6 (m/s)/m were seen but these gradients were much smaller at depth. An rms misfit was used to evaluate the fit of the model to the data:

$$rms\ misfit = \sqrt{\frac{1}{N}\sum_{i=1}^{N}\left(\frac{TT_{calc,i} - TT_{obsv,i}}{TT_{error}}\right)^2}$$

where TT is the travel time and TT_{error} is the estimated uncertainty for each of the N travel times from the records. An rms misfit of 1.0 would indicate that the data are fit only to the level of the errors in the data. The rms misfit for the S-wave model in Figure 15 was 0.770, indicating that the data were fit to below the level of estimated errors. While the S-velocity model shows considerable lateral and vertical variation (Figure 15), we are interested primarily in an average velocity in the upper 30 m. MacRay (the forward modeling program) generates a block model of the velocity structure with blocks 10-m wide by

1-m thick. We then compute the vertical travel time through each 10-m wide column:

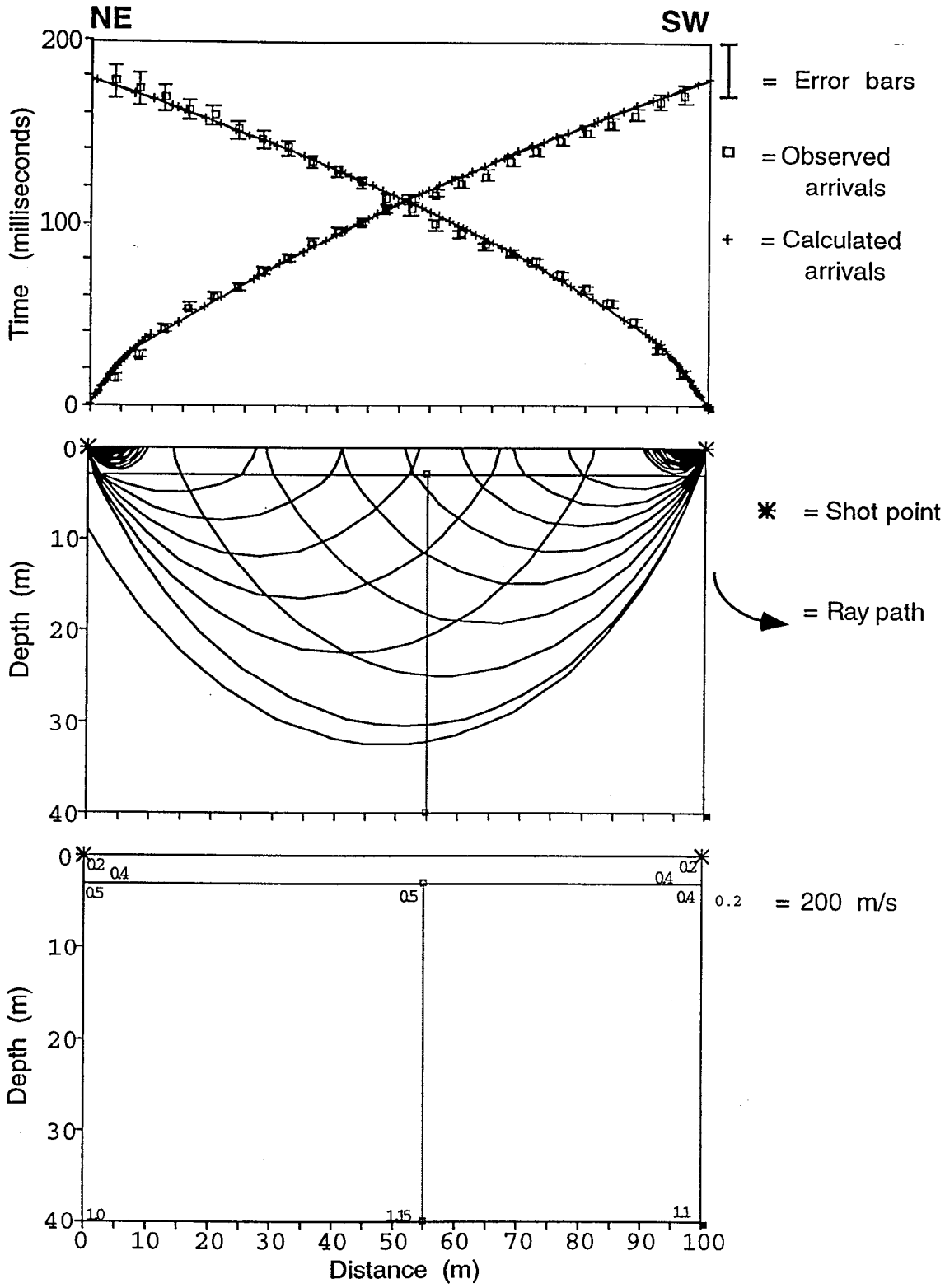

Figure 14 - P-wave results from line 11. Average rms misfit = 0.949. Average P-wave velocity = 757 m/s.

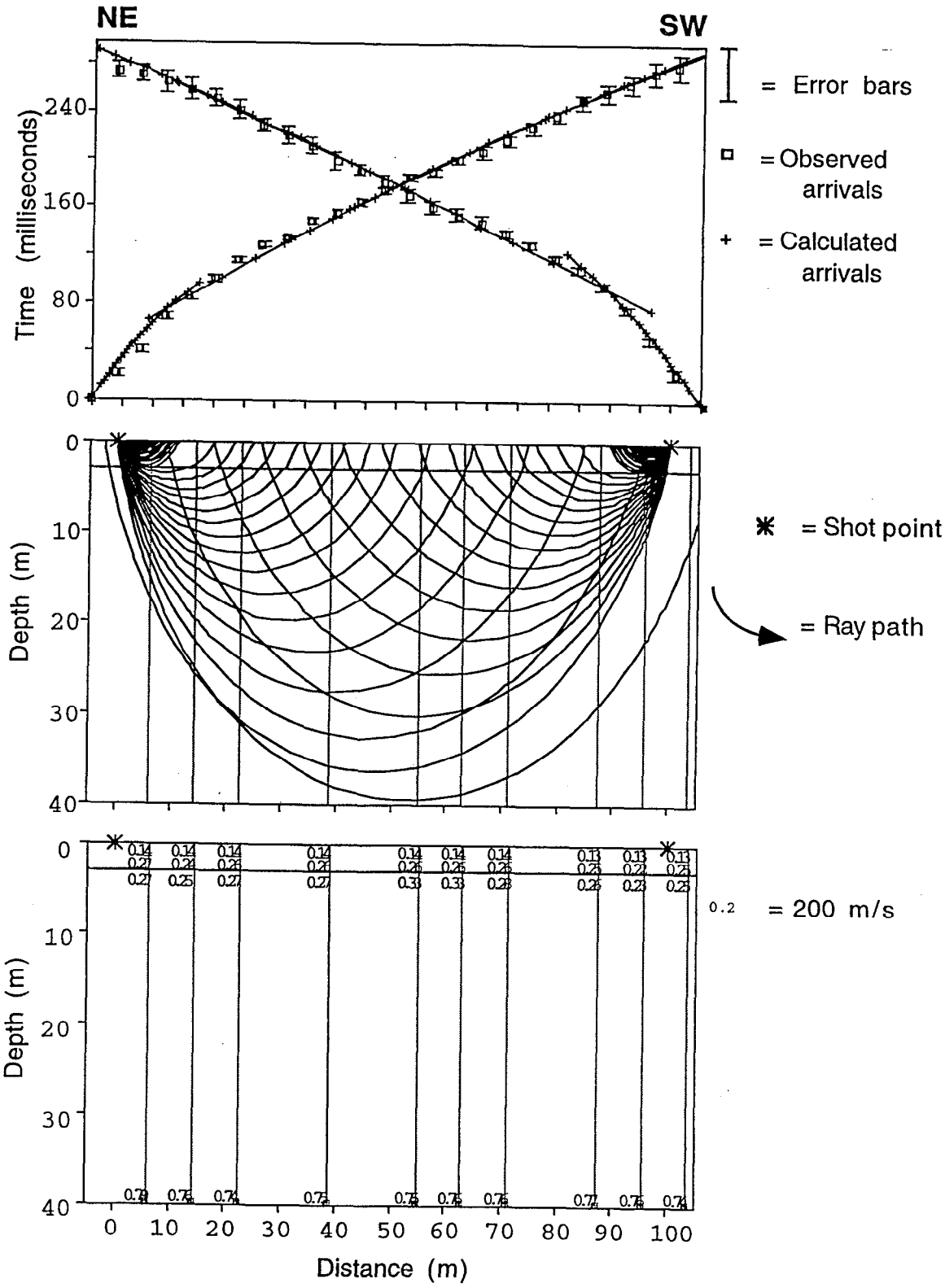

Figure 15 - S-wave results from line 11. Average rms misfit = 0.770. Average shear-wave velocity = 491 m/s.

$$V_S ave = \frac{d}{\int_0^d \frac{dz}{v(z)}} \quad , \tag{2}$$

where d=30 m and $v(z)=v_0$ in a layer with no gradient and $v_0 + gz$ in a layer with a gradient. The average travel time is then computed from vertical travel times through each column, and that average is divided into 30 m. The result is the average shear-wave velocity for a wave passing vertically through the uppermost 30 m of the section. This average for the line in Figure 15 is 491 m/s. The average velocities for the 13 seismic lines are then compared to soil type to determine if the soils have statistically different responses (Table 3). The logarithmic average of velocities within the Ramona unit is 637 ± 198 m/s, while the average for the Madera unit is 494 ± 77 m/s. (The measurement in the Hanford unit is not included in either average because the average of 491 m/s represents a mix of the Hanford soil in the upper 3 m (Figure 10) and either the Ramona or Madera unit below 3 m. With the wide range of velocities in the Ramona soil, are these two units different? We use a modified Student's T-test (Press et al., 1992) to test the possibility that these two distributions could be subsamples of the same distribution. The T-test yields a significance, which is the probability that the two distributions could be the same. The modified T-test for the Ramona and Madera soils yields a probability of only 14% that these two units could actually be drawn from the same master distribution. We therefore conclude that the Ramona and Madera soils have statistically different seismic response. We have assigned the average velocity of the Madera soil (494 m/s) to the Hanford unit (Figure 16) because that unit is

Table 3 - Average Shear Wave Velocities and Soil Types

Line Number	$V_{s,ave}$,m/s	Soil Type
1	428.0	Madera/Ramona
2	434.0	Madera
3	487.0	Madera
4	483.0	Ramona
5	636.0	Ramona
6	512.0	Madera
7	741.0	Ramona
8	541.0	Madera
9	973.0	Ramona
10	560.0	Ramona
11	491.0	Hanford/Madera
12	634.0	Madera
13	426.0	Madera

Table 4 - Comparison Between Shear-Wave Velocities from Seismic Lines and Borings

Depth, m	UCR-2 V_s, m/s	Line 4 V_s, m/s[1]	UCR-3 V_s, m/s	Line 1 V_s, m/s	Vel Log V_s, m/s[2]
1.52	186	250	229	270	-
3.02	264	310	254	350	273
4.57	323	360	324	360	355
6.07	412	410	304	370	396
7.56	496	530	376	390	368
9.11	642	560	404	400	340

[1] This line had large lateral variations in velocity at the southern end; the boring was projected into the line and velocities picked along a vertical profile 20 m north of the end of the line.

[2] These velocities are from the suspension log in UCR-5 (100 m deep borehole).

so thin and because the Madera is found both north and south of the Hanford soil (Figure 8).

3.5 Cone Penetrometer Testing

Characterization of the immediate geotechnical environment around Rivera Library included cone penetrometer tests (CPT) in four borings around Rivera Library (see inset in Figure 8). CPT tests measure the resistance to forcing a probe into the soil and frictional resistance along the sides of the probe (Figure 17). The cone bearing force, Qt, and the friction ratio, Rf, are used to classify soils (Gregg In Situ, 1997). These borings (Figures 18-21) show generally that the upper 30 m (100 feet) consists of thin, interbedded silts, sands, and clays with weak soils in the upper 3-6 m (10-20 feet). At greater depths, the percentage of stiff, fine-grained soils and cemented sands increases. Comparisons between the borings reveal that the gross stratigraphy is continuous between borings 100 m apart but vary on scales of 300-400 m. Stratigraphy in borings UCR-1 (Figure 18) and UCR-2 (Figure 19) is similar once the log for UCR-1 is shifted up 1.5 m (5 feet) to account for the elevation difference between these two borings. While the borings UCR-3 (Figure 20) and UCR-4 (Figure 21) are similar, they both differ from either UCR-1 or UCR-2. In addition to the geotechnical data provided by these borings, they also establish that the stratigraphy is laterally continuous over distances of 100 m but discontinuous at distances of 300 m.

Measurements of the shear-wave velocity were also taken at borings UCR-1, UCR-2, and UCR-3. Based on differential travel times between points in the boring, interval velocities were calculated. Velocities can be compared between these borings and the seismic lines. Velocities

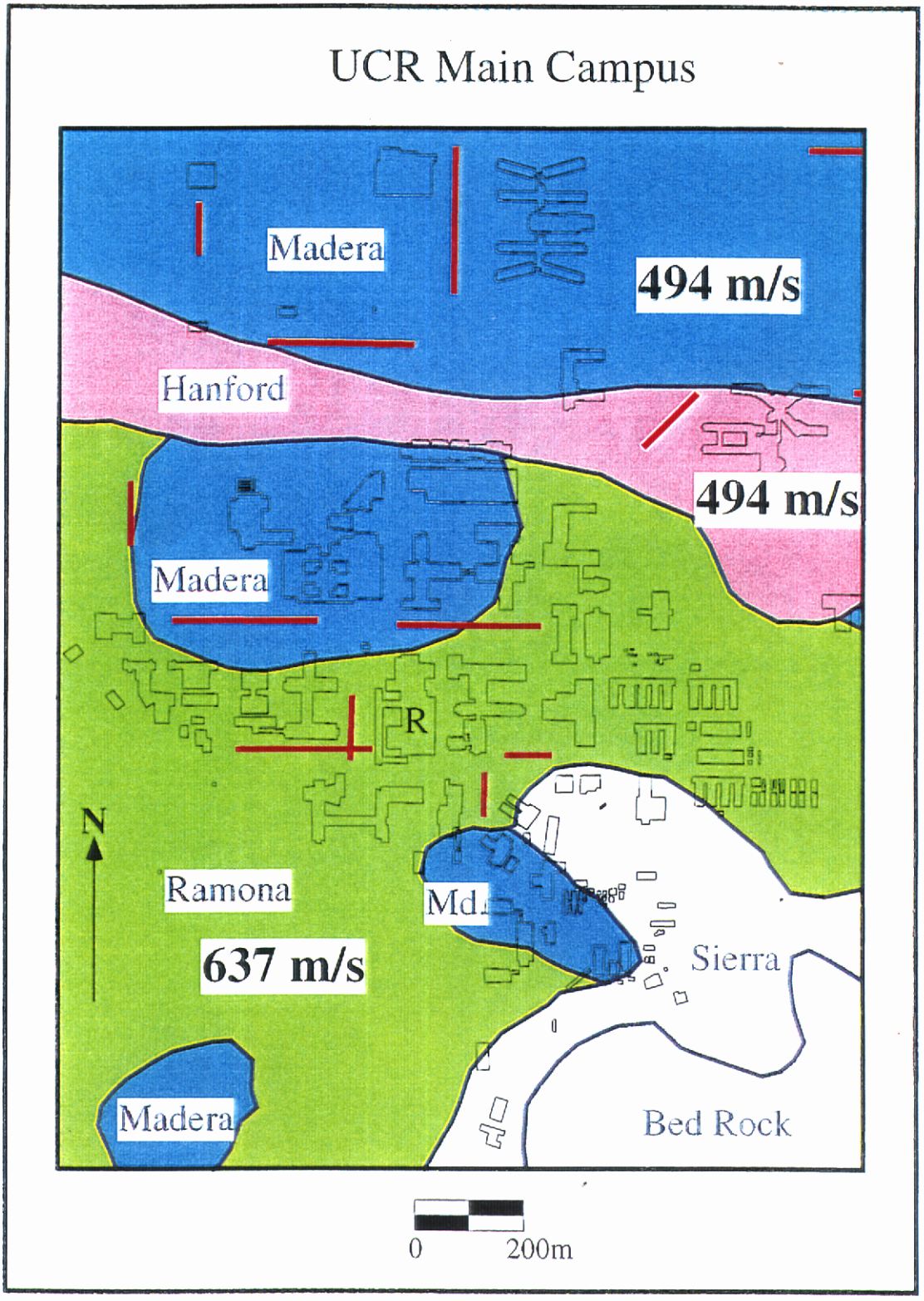

Figure 16 - Map of UCR campus with average shear-wave velocities for the upper 30 m assigned to soil units. See caption of Figure 8 for explanation of other symbols.

Figure 17 - CPT testing system at UCR-2. The weight of the truck (20 tons) provides the driving force for the probe.

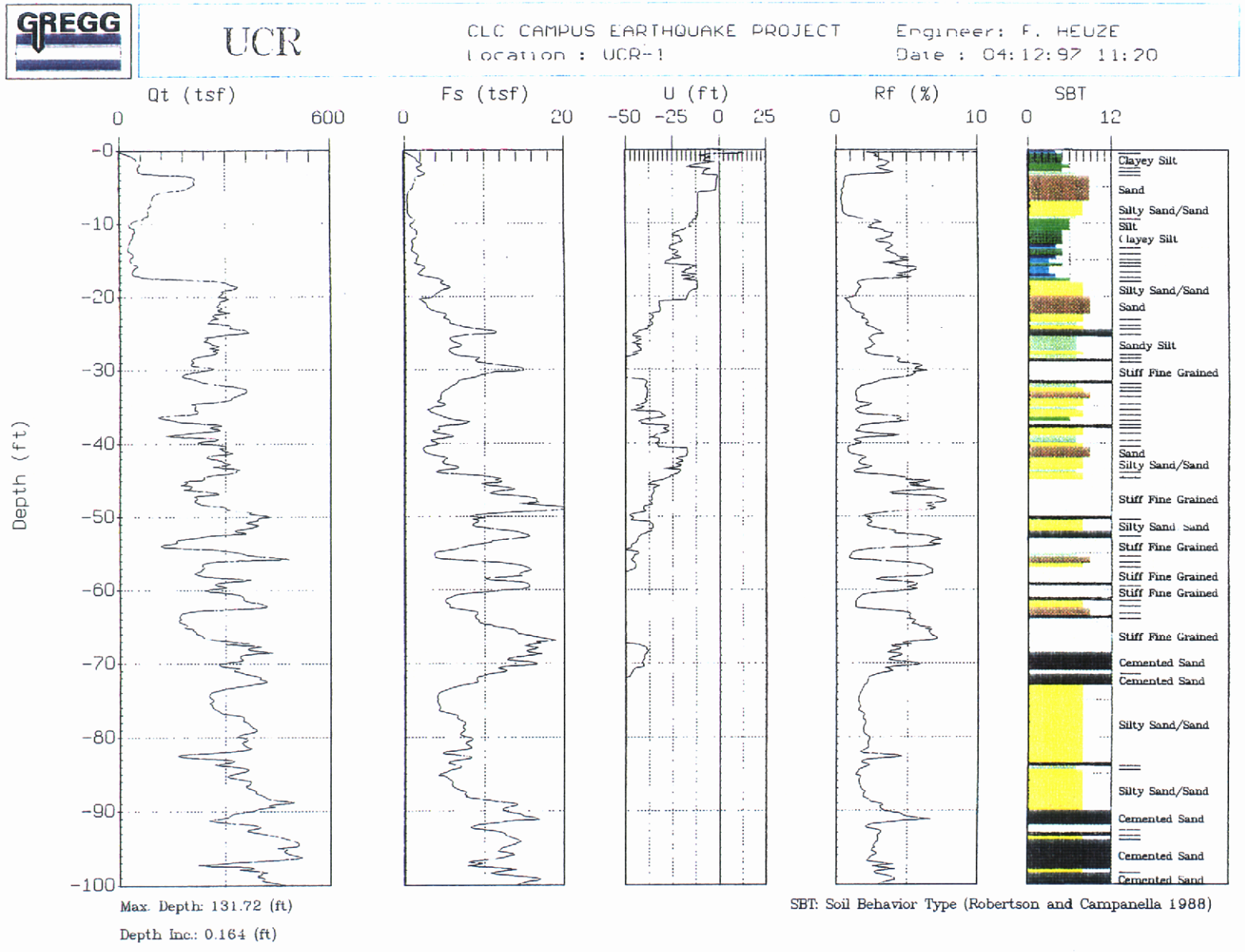

Figure 18 - Cone Penetrometer log for UCR-1.

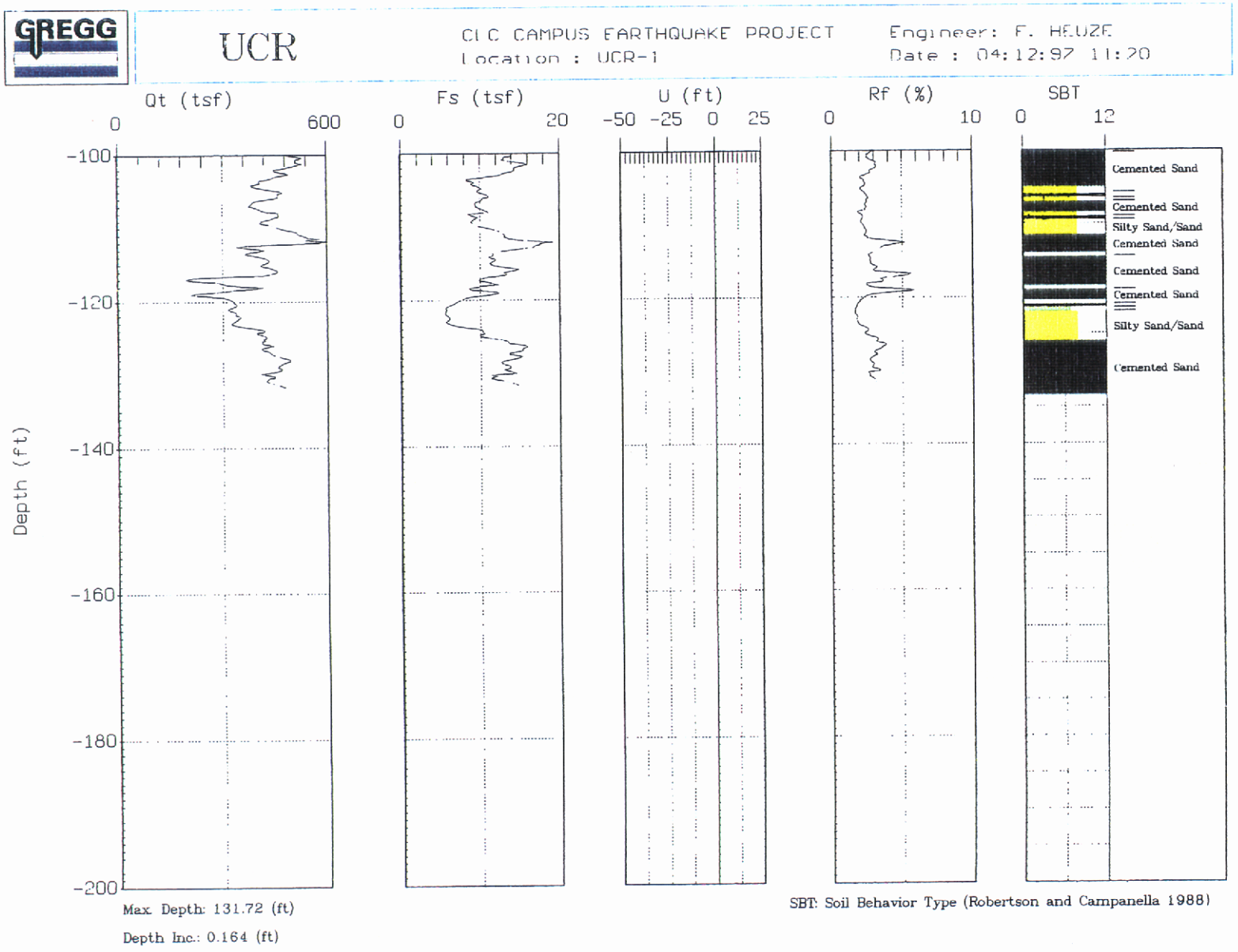

Figure 18 - continued.

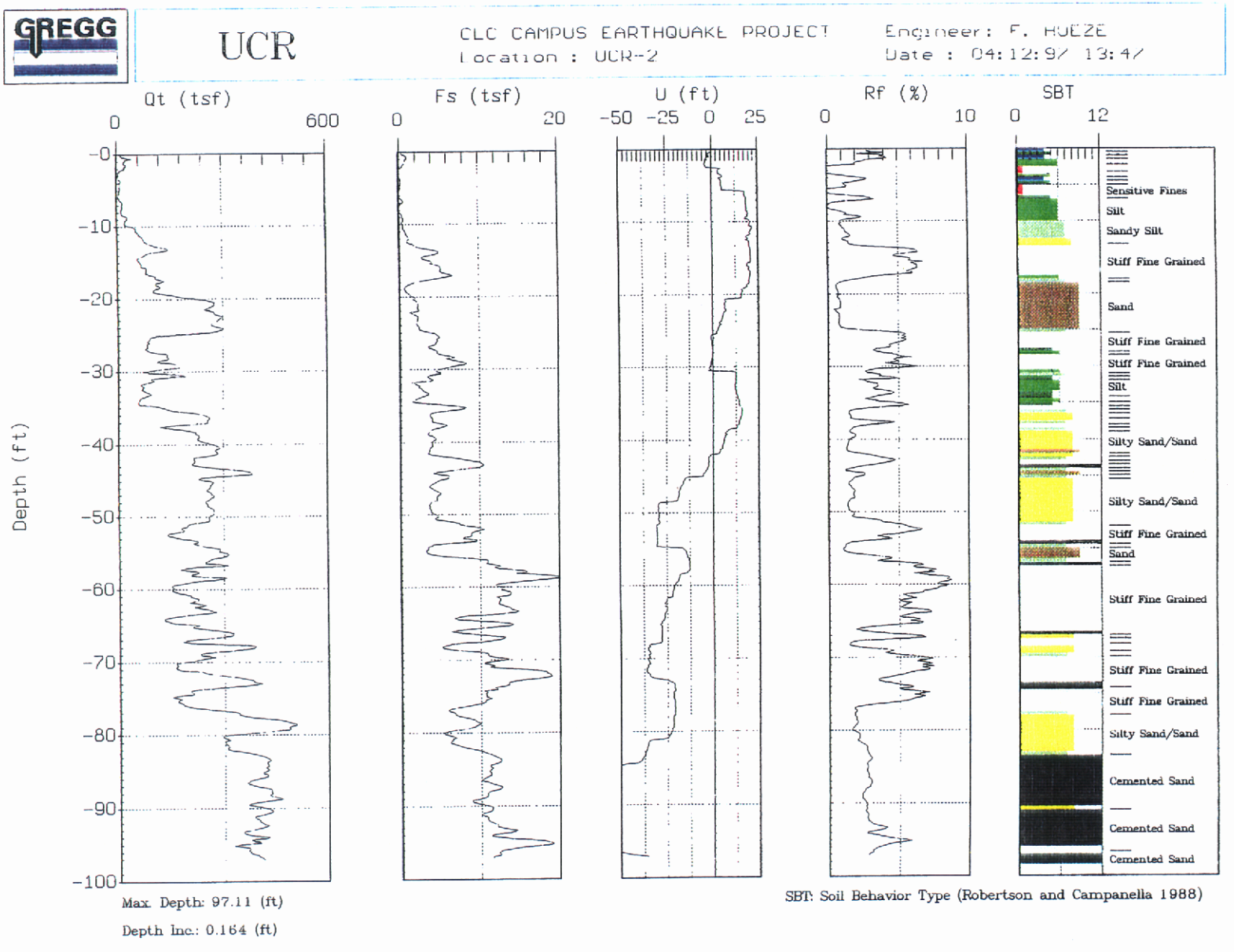

Figure 19 - Cone Penetrometer log for UCR-2.

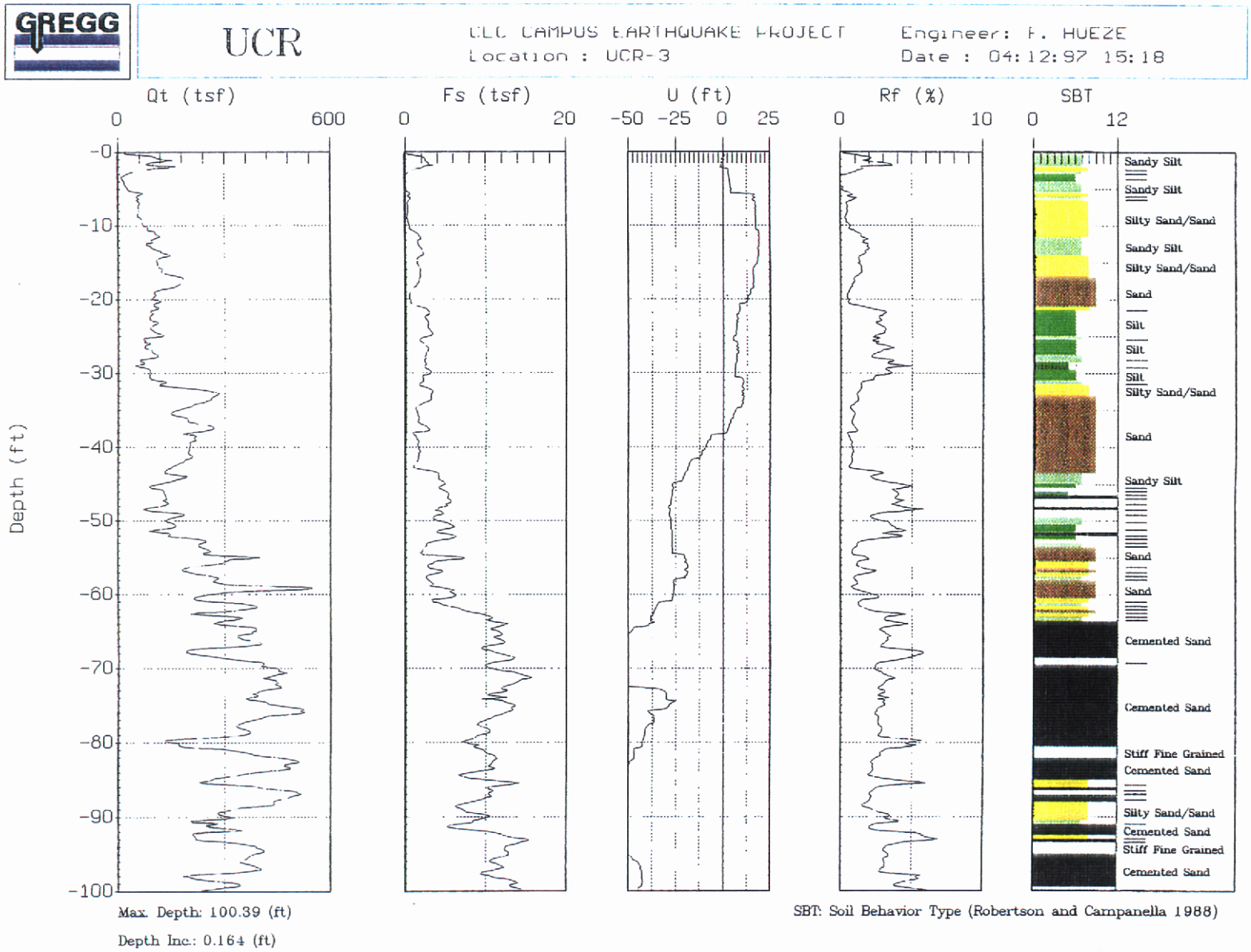

Figure 20 - Cone Penetrometer log for UCR-3.

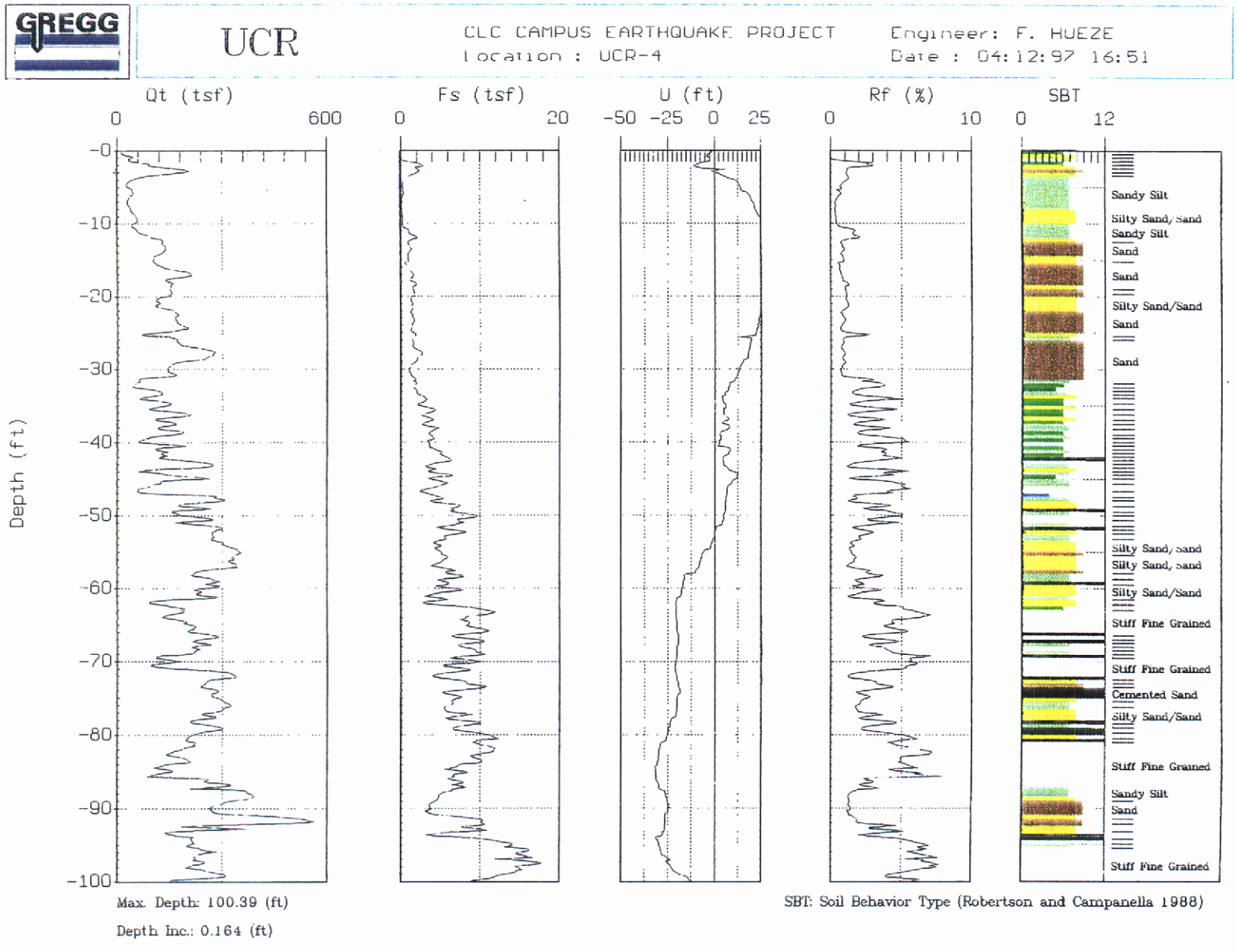

Figure 21 - Cone Penetrometer log for UCR-4.

between UCR-2 and Line 4, and between UCR-3 and Line 1, were compared (Table 4). In general, the velocities are comparable (usually within 10%) except near the surface. Within the first 3 meters, the refraction profiles tend to overestimate the velocities. However, overestimation for 10% of the the 30-m transit distance will not affect the average velocity significantly (Park and Elrick, 1998). The refraction profiles have the added advantages of lower cost and sampling a larger volume than the borings.

3.6 Geophysical Logging

A suite of geophysical logs were run as part of the program to characterize the vicinity of the seismic station. They were performed in the 100 m deep borehole (UCR-5; Figure 8) in which bedrock was encountered. These logs included several resistivity measurements, self potential, gamma ray, and both Vp and Vs suspension logging (Figure 22). Details of the resistivity, self potential and gamma ray logs are contained in Welenco (1998), while the velocity logs are discussed in Geovision (1998). The most obvious lithologic contrast in the logs is between the sediments and weathered bedrock, where the resistivity increases rapidly by an order of magnitude at a depth of 88 m and both Vp and Vs almost double (Figure 22). The constant increase in resistivity from depths of 88 m to 94 m, as well as the highly variable velocities in this zone, indicates weathered bedrock. The interpretation of bedrock below a depth of 94 m is based largely on the high resistivities and the decrease in rates of drilling below 94 m; no velocities were available for this segment of the borehole.

The water table is interpreted to be at a depth of 70 m where Vp increases by 60% while Vs shows no increase. Surprisingly, the resistivities exhibit only a 20% decrease at this depth

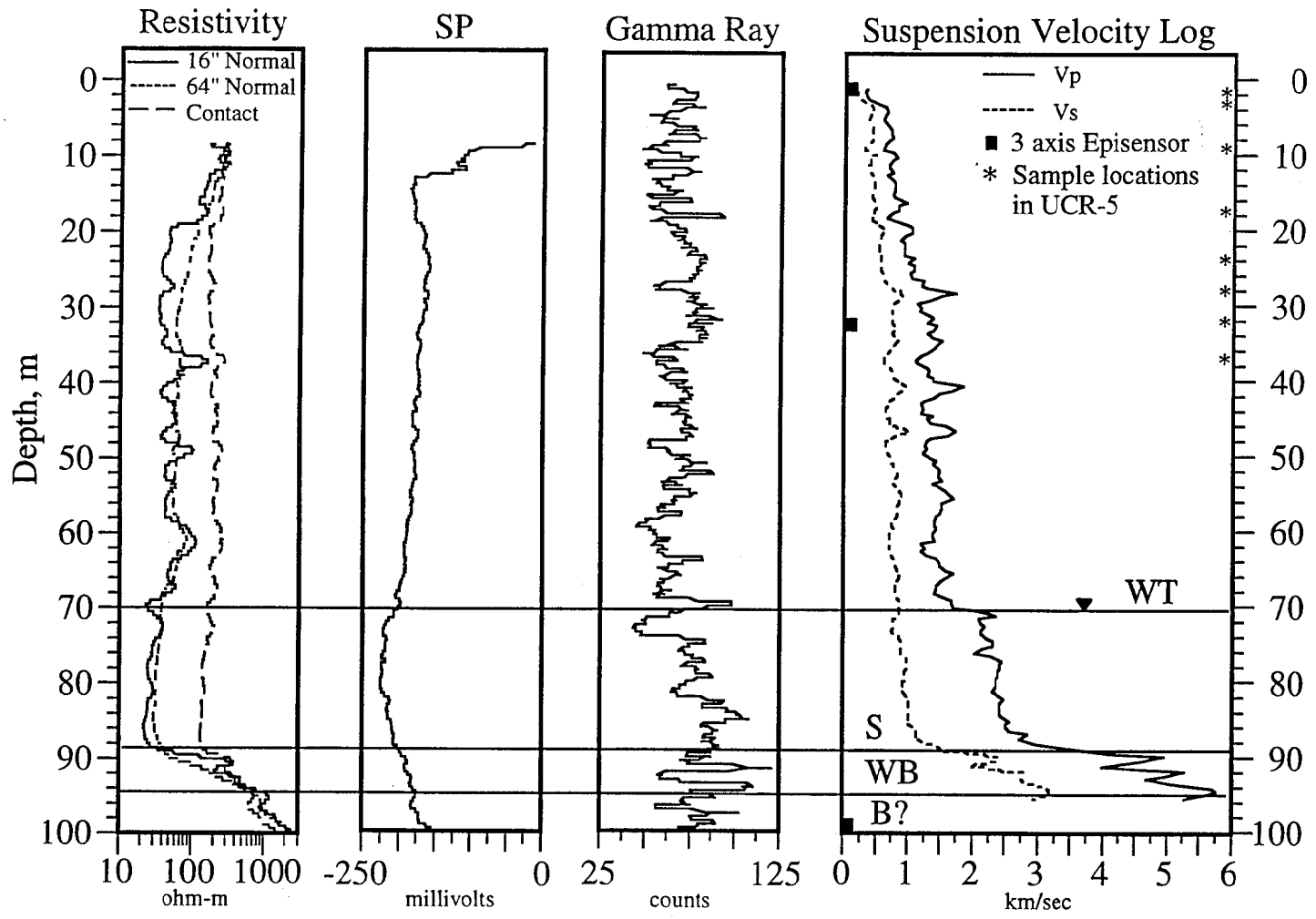

Figure 22 - Geophysical logs from 100-m deep borehole (UCR-5). Water table is shown as a rise in P-wave velocity with no S-wave velocity change (WT), and contact between weathered basement (WB) and sediments (S) is shown by rise in resistivities and seismic wave velocities. Location of seismometers shown on velocity log. Contact between basement (B) and weathered basement is inferred from change in drilling rate (see text).

(Figure 22). Normally, the transition from undersaturated to saturated conditions is marked by a substantial resistivity decrease (factor of 2 or more) because ionic conduction through the fluid is the dominant process. The slight decrease is evidence that either the sediment is water-wet throughout most of the column below 18 m (where the resistivity drops appropriately by a factor of 2 or more) or that surface conduction along clays plays a key role in conduction (or both). Evidence of thin layers is apparent in the velocity, resistivity, and self potential logs, but there is little correlation between these thin zones of changing material properties. On the basis of a change in the velocity gradient at a depth of 30 m, we have tentatively identified two sediment layers (Figure 23). The upper one has a gradually increasing P wave velocity from 0.5 km/s at 4 m depth to 1.4 km/s at 30 m, and the lower one has a relatively constant velocity of 1.4 km/s. It is possible that this is a single layer with a lower compacted zone, however. There is no clear stratigraphic layering in the sediments above 88 m, an observation consistent with the alluvial source of the sediment and its proximity to the source outcrops. The lithologic log of the hole, based on cuttings brought up in the mud, confirms the general lack of clear sediment layering (Table 5).

The shear-wave velocities from the suspension logs are very similar to those from the nearest seismic refraction line (Table 4). While velocities from the refraction survey are higher than those from either log in the upper 3 m, agreement is good at depths from 3-7.56 m. The velocity value at a depth of 9.11 m is approximately 20% higher than that from the suspension log (Table 4). In general, the differences between the suspension log and the refraction profile are comparable to those between the log and the velocities measured with the CPT testing. Again, refraction appears to be an accurate method of determining shallow shear-wave velocities and is

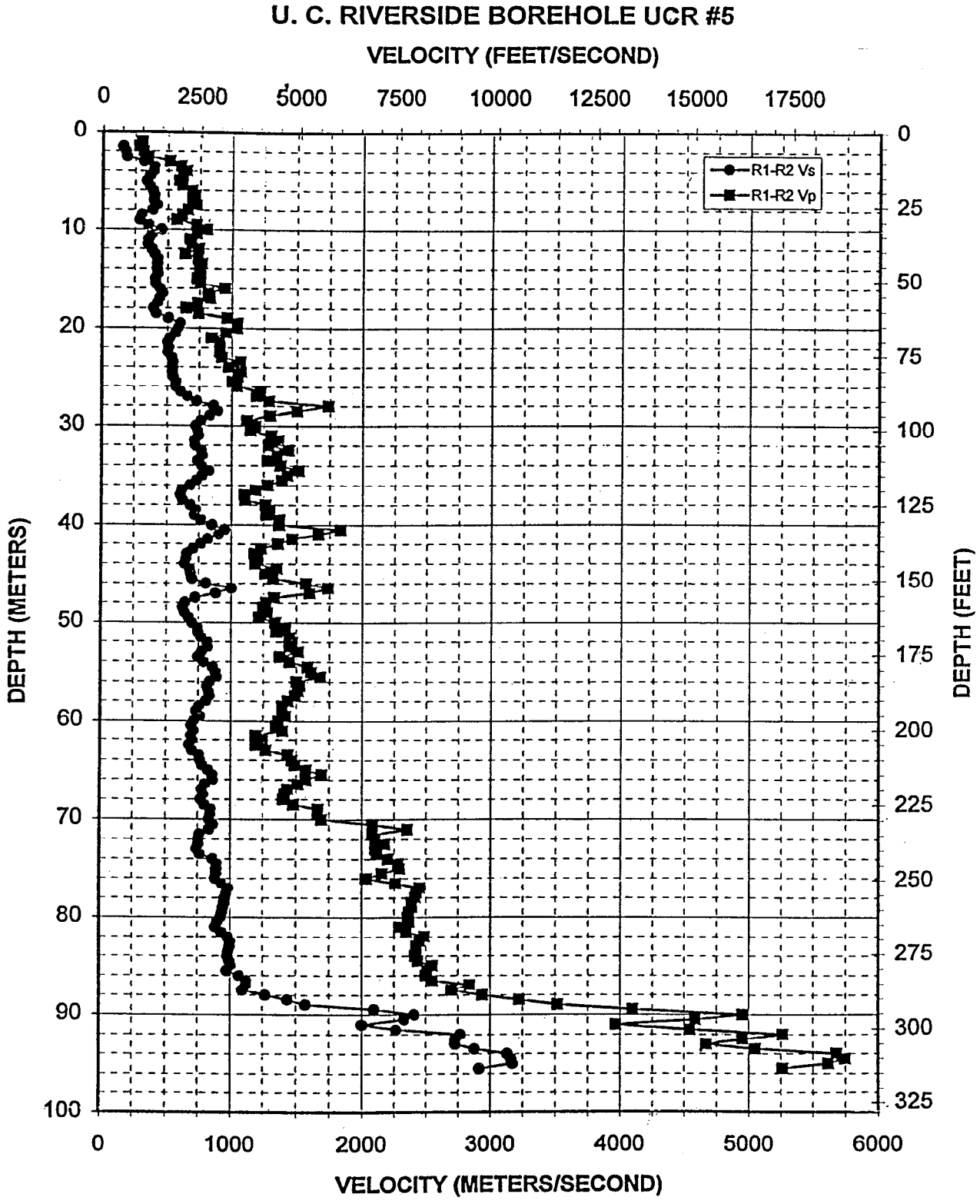

Figure 23 - Suspension logs of P-wave and S-wave velocities . Data points sampled every 0.5 m.

Table 5 - Lithologic Log of UCR-5, from Jeff Wagoner's and Stephen Park's notes.

Depth	Observations
0-12.2 m	Rapid drilling, weak arkosic sand
12.2-12.8 m	Finer sediments
12.8 m	Sandy
18.3 m	Sediment becomes denser and finer grained
18.9 m	Thin clay beds (?)
26.2-28.0 m	Clayey sand
48.8 m	Coarse-grained sand (?)
88.1 m	Bedrock (Drilling rate decreases from 9 to 2.3 m/hour)
94.8 m	Drilling rate decreases to 0.6 m/hour.
99.7 m	TD in bedrock

Table 6 - Directional Survey for UCR-5

Depth, m	Inclination, Degrees	Direction, Degrees
6.1	0.1	240
12.2	0.1	240
18.3	0.1	240
24.4	0.3	222
30.5	0.4	229
36.6	0.4	250
42.7	0.3	290
48.8	0.3	42
54.9	0.7	353
61.0	0.8	352
67.1	0.7	320
73.2	1.0	317
79.2	1.1	292
85.3	0.5	318
91.4	1.4	267
93.0	1.8	259
94.5	2.1	261
96.0	3.0	259
97.5	3.5	258
98.5	3.3	258
99.1	3.5	261

much less expensive than borehole logs.

A directional survey was also run in the deep borehole in order to determine its deviation from vertical. This survey is summarized in tabular form (Table 6) and shows that there was a maximum deviation of 3.5° at the bottom of the hole. Prior to penetration into bedrock, this deviation was consistently less than 1.1°. The bottom of the hole is offset approximately 0.9 m from true vertical, for an average deviation of 0.5°.

3.7 Seismic Station Instruments and Installation

A central component of this seismic hazard study was the installation of borehole and surface seismic sensors for the study of how ground motions are actually experienced on the campus. Three sensors were installed at the north end of Rivera Library in holes UCR-5 (100-m deep borehole) and UCR-6 (31-m deep borehole), and at the surface (Figures 24, 25). The Kinemetrics Episensor (FBA ES-T) force balance accelerometer was used for all three locations (Figure 26). This triaxial unit is capable of recording accelerations as small as a few μg and as large as 2.0 g. The downhole units contain Episensors in a sealed borehole package (Figure 27). The downhole instruments were installed in the boreholes, which were then filled with cement to within 3 m of the surface. The cable from the shallow borehole (UCR-6) was run through a 2" diameter PVC pipe buried 46 cm (18") deep back to the deep borehole (UCR-5). A 4" diameter

PVC conduit was run from UCR-5 in a 1-m (~36") deep trench back to an electrical installation box at the northeast corner of Rivera Library. Then, a 15-cm thick concrete pad was poured at

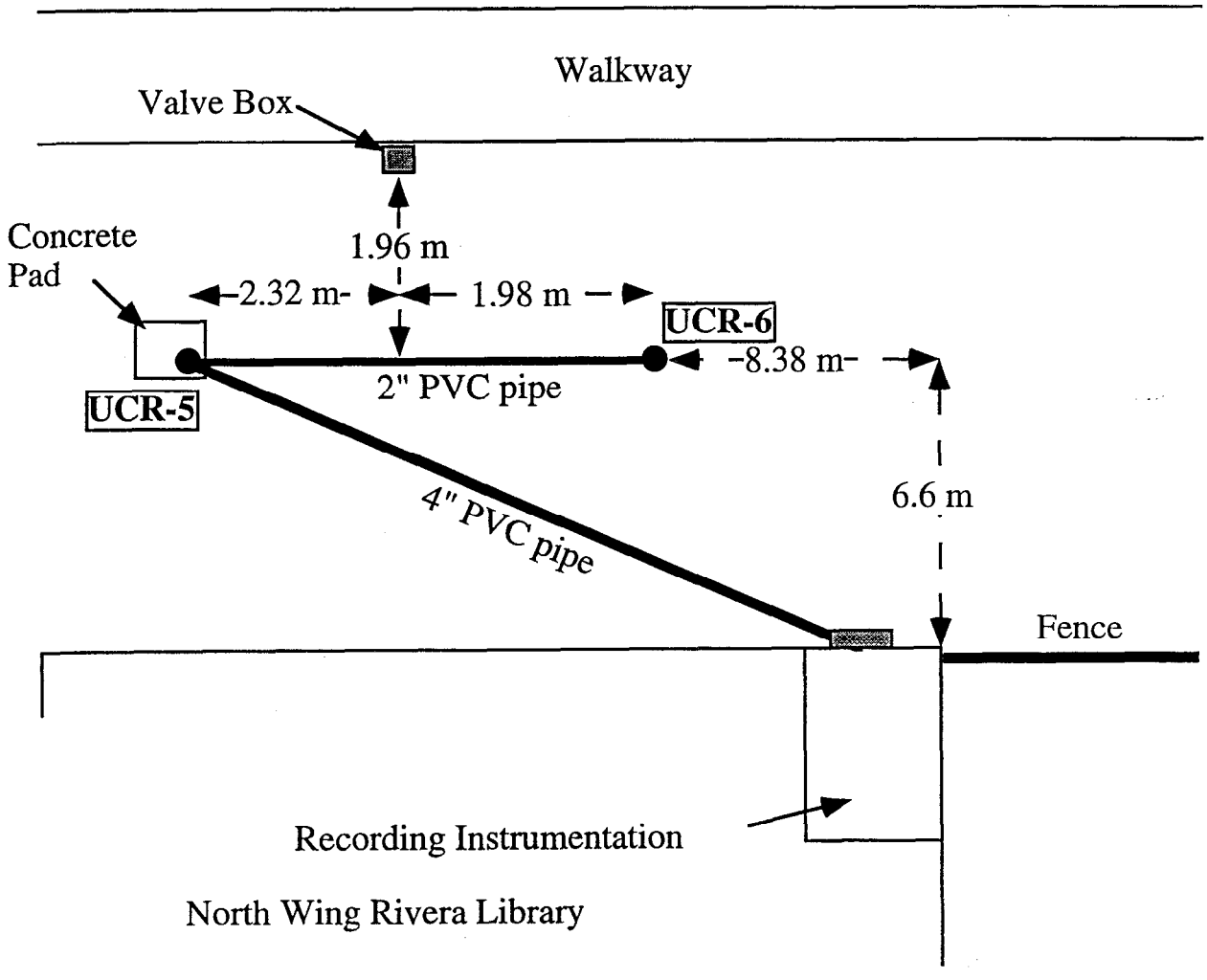

Figure 24 - Schematic map of the UCR seismic station installation (drawing not to scale). The 2" (5-cm) diameter PVC pipe is in a trench 0.46-m deep, while the 4" (10-cm) diameter PVC pipe is in a trench 0.61-m to 1-m deep.

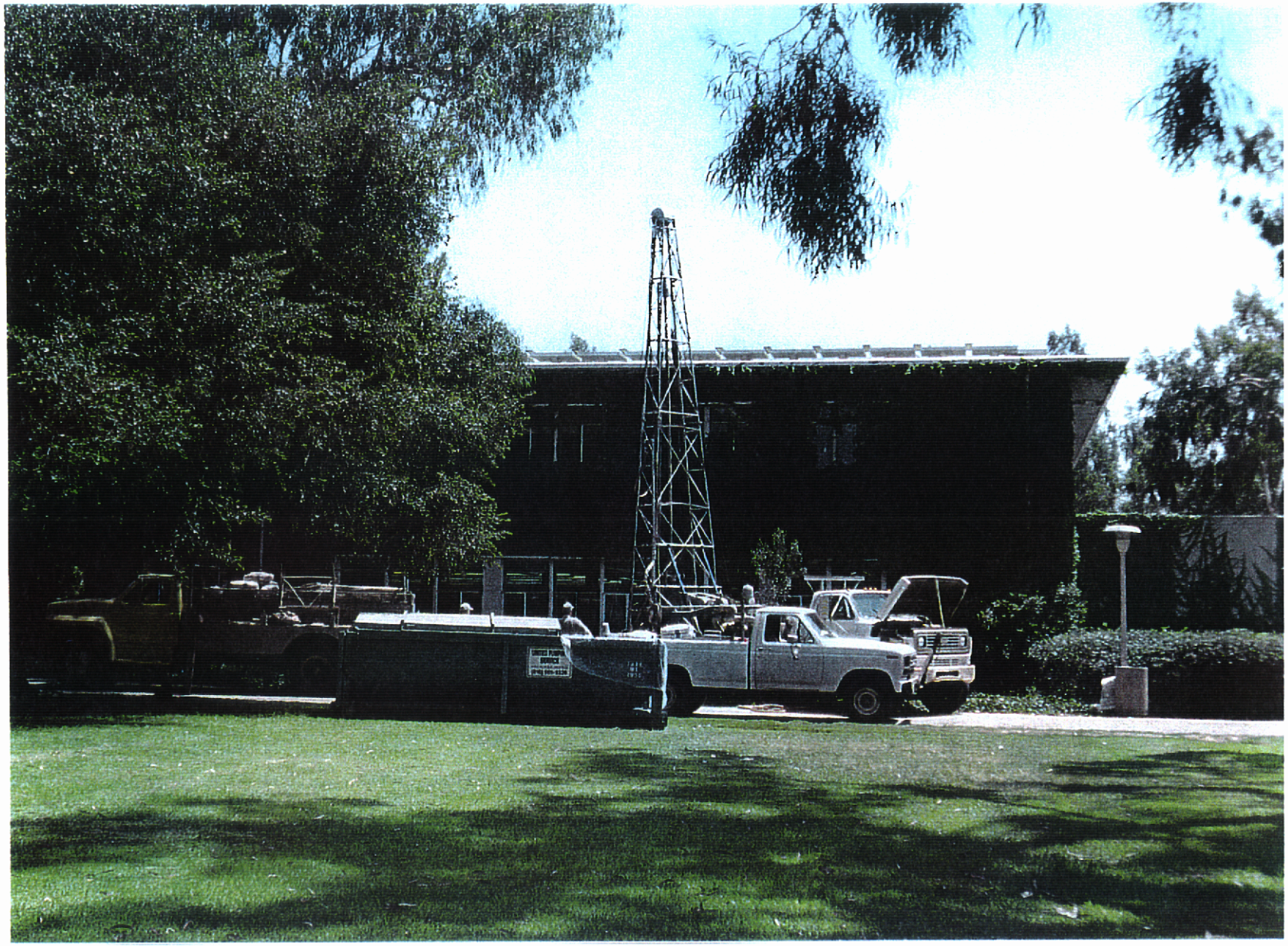

Figure 25 - Drilling the deep borehole at the north end of the Rivera Library (UCR-5).

Figure 26 - Surface seismic sensor, on left, and downhole seismic sensor, on right, in its test housing.

Figure 27 - Downhole seismic sensor, as it is prepared to be lowered into UCR-5.

the top of UCR-5 for the mounting of a waterproof box. Once this box was installed, the surface Episensor was mounted to the cement pad with a concrete anchor. All cables were passed through the larger conduit back to Rivera Library where the recording instruments are located (Figure 24). The Episensors are connected to Quanterra 4128 24-bit seismic dataloggers. Timing is provided by internal clocks which are continually updated by signals from a GPS receiver mounted on the roof of Rivera Library. Once the installation is complete, there will be two units with a total of 12 channels (3 spare channels and 9 used for the deep, shallow, and surface sensors). Both recording units are connected via real-time Ethernet links to the Trinet data center run by the USGS (**http://www.trinet.org/scsn/scsn.html**) and to the IGPP data center at UCSD (**http://epicenter.ucsd.edu/ANZA/home.html**). Currently, all sensors are telemetered. Additional characteristics of the Rivera installation site are given in Table 7.

Table 7 - Seismic Instrumentation at the UC Riverside CLC Station

Channel	Borehole	Depth	Orientation	Geology
	(Episensor DH SN101)			
RSB HLE	UCR5	99.1m	354°MN	Bedrock
RSB HLN	UCR5	99.1m	264°MN	Bedrock
RSB HLZ	UCR5	99.1m	Vertical	Bedrock
	(Episensor DH SN102)			
RSB HLE	UCR5	31.9m	345°MN	Sediment
RSB HLN	UCR5	31.9m	255°MN	Sediment
RSB HLZ	UCR5	31.9m	Vertical	Sediment
	(Episensor ES-T SN119)			
RSB HHE	UCR5	0.0m	180°N	Surface
RSB HHN	UCR5	0.0m	90°N	Surface
RSB HHZ	UCR5	0.0m	Vertical	Surface

3.8 Initial Recordings at the New UCR Station

A M4.5 earthquake on October 1, 1998 near Big Bear was recorded on both the surface and deepest borehole sensors shortly after the Riverside station began collecting data. Maximum accelerations of 0.01 g (10 cm/s^2) were recorded at the surface with accelerations 10 times smaller within bedrock (Figure 28). A second earthquake with a magnitude of 4.9 was recorded on October 27, 1998. Comparison of the downhole and surface records confirmed the approximate peak acceleration amplification factor of 10 (Figure 29). Such a large amplification factor was predicted for strong ground motions in Riverside in the Seismic Safety Element (Envicom and County of Riverside, 1976). Surface motions are strongly influenced by the properties of the top 30 m of the soil column. This is why we are making special efforts to characterize that part of the soil profile.

From the records of the earthquake on October 27, 1998, we have determined a spectral acceleration amplification curve. We compare it to the one provided by Envicom and the County of Riverside (1976) in Figure 30. The dashed line is the spectral relation predicted by Envicom and the County of Riverside for a generic site in the city of Riverside. This shows relative amplifications for different frequencies (1/period) of seismic waves and was computed in an empirical fashion from an observed record in El Centro for the 1940 Imperial Valley earthquake. The solid line is the calculated spectral amplification for the Rivera station using the weak motions recorded on October 27, 1998. While both curves are relatively similar at periods longer than 0.4 s (e.g., frequencies lower than 2.5 Hz), there are substantial differences between periods of 0.1-0.4 s. Our recorded spectrum shows a strong peak near 0.3 s where the Envicom estimate shows a low value, and the opposite is true at a period near 0.2 s. None of the recorded spectral

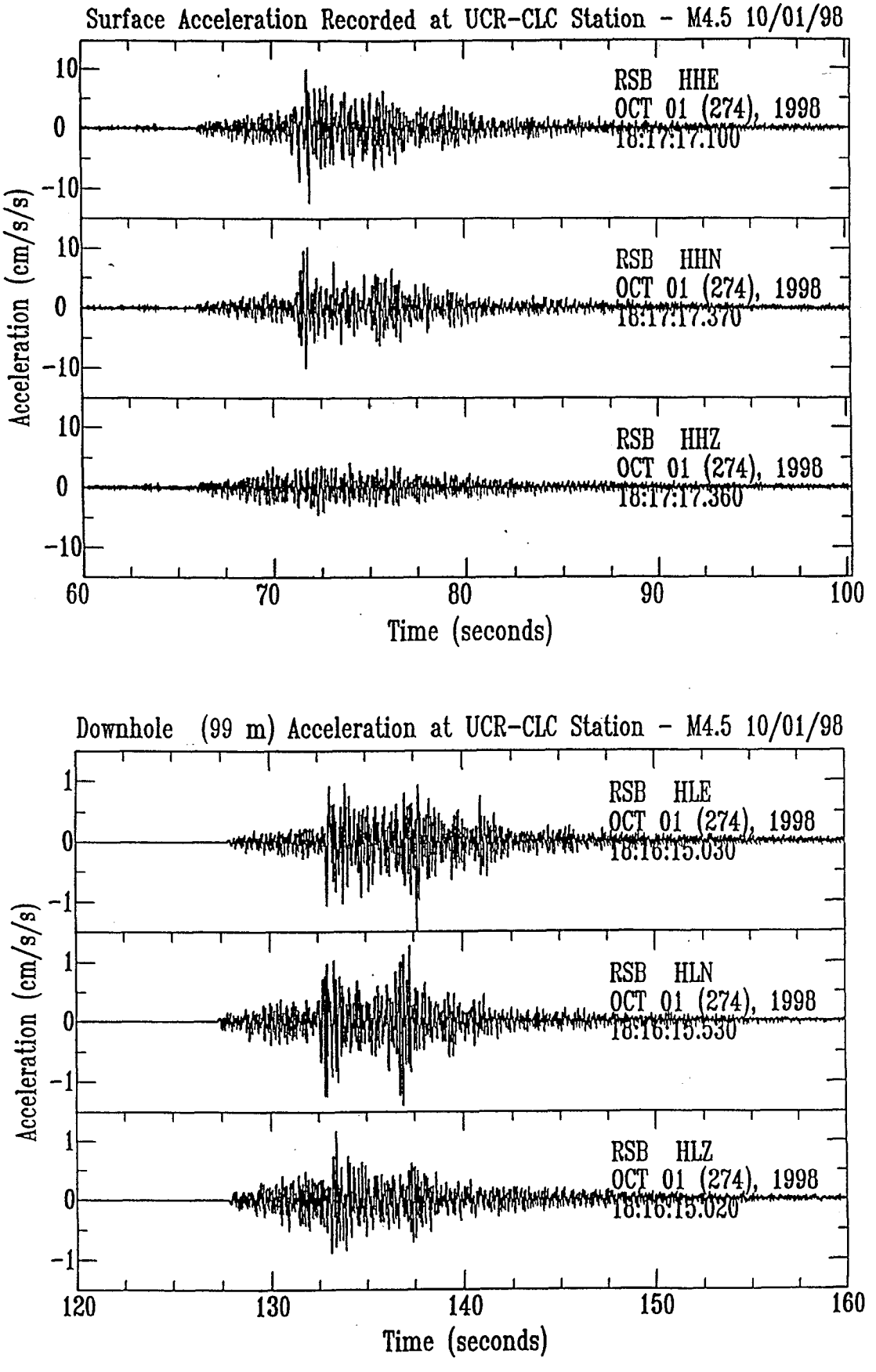

Figure 28 - UCR surface and 99-m deep records of M 4.5 event on 10-01-98, near Big Bear, CA.

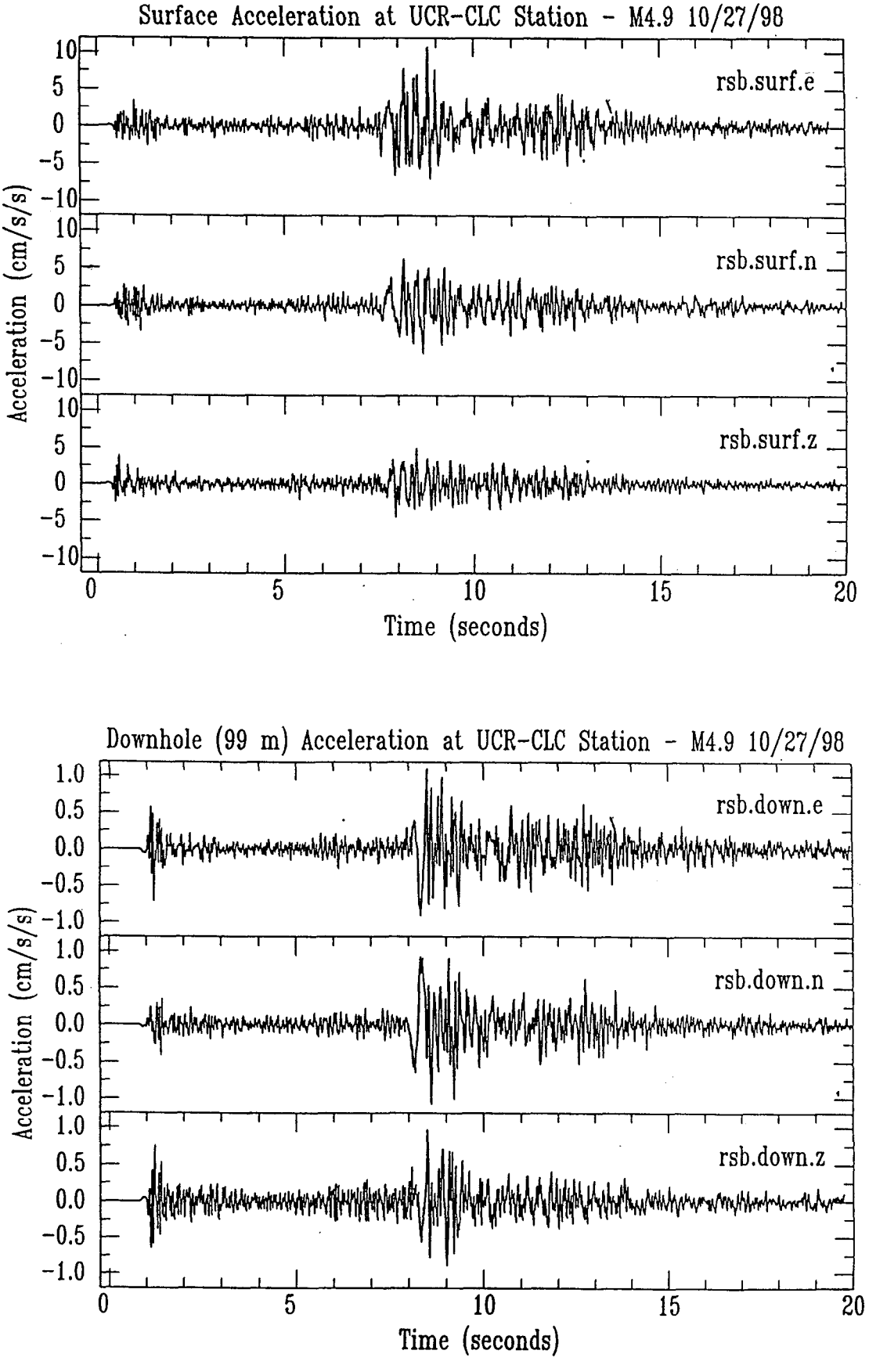

Figure 29 - UCR surface and 99-m deep records of M 4.9 event on 10-27-98, near Big Bear, CA.

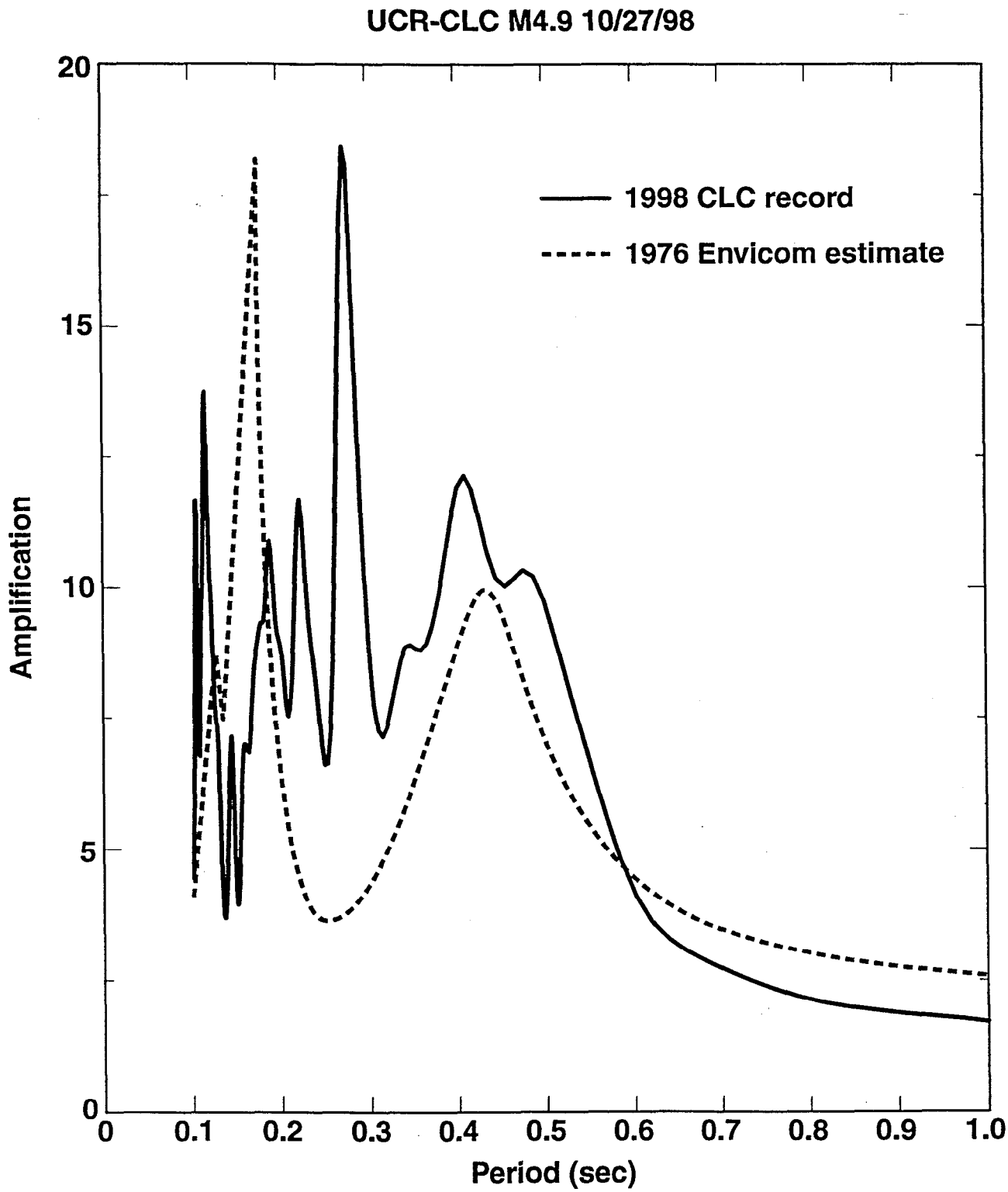

Figure 30 - Comparison of acceleration spectral amplification between 99-m depth and surface at UCR for weak motions, to predictions from Envicom report (1976) for strong motions.

amplifications are much below factors of 5-7 in this range, however. These peaks are important because, to a first approximation, the natural period of a building is (# stories) x 0.1 s. Thus, a three-story building would have a natural period close to our recorded peak near 0.3 s. Such a high spectral peak at this period should be considered carefully when designing structures where the Long Range plan limits building height to below the trees (typically 3 stories). This difference between the Envicom report and our computed spectrum shows the utility of monitoring ground motions to the safe design of buildings on the UCR campus. It is important to note that the estimates from the UCR seismic station are for weak motions, and strong motions from large earthquakes may behave differently.

The modeling described in Section 1.1 will yield the appropriate strong motion amplifications for UCR.

4.0 CONCLUSIONS

The University of California, Riverside campus lies close to two of the most active faults in southern California. The San Jacinto fault to the east and the San Andreas fault to the north are both capable of generating ground accelerations exceeding 0.2 g with appreciable probabilities over the next 30 years. Therefore, the campus has a high risk of experiencing potentially damaging earthquakes. This risk is exacerbated by the local geologic conditions, which consists of silty sands and clayey sands overlying granitic basement (Matesic and Vucetic, 1998). The contrast in shear-wave velocities and densities between the sediment and basement results in local peak acceleration amplifications of approximately 10, as observed in earthquakes in late 1998. A seismic hazard study of the University of California, Riverside campus had resulted in mapping regions of higher and lower shear wave velocities. In combination with the variable depth of the soil column, this should create regions of significantly different intensities of ground shaking on the campus in large earthquakes. Different soil types on the campus show statistically distinct shear-wave velocities and are therefore geotechnically distinct units. Gravity measurements coupled with the borehole logs at UCR-5 reveal depths to basement beneath the campus of at least 90 m and possibly as much as 150 m. The new installation of three triaxial accelerometers within basement, within the sediment, and at the surface now permits monitoring of ground motions as they traverse the sedimentary column. These observations will allow the development of quantitative predictive models of ground motion which are specific to the UCR campus and will better estimate the variability of that motion across the campus. A continuing study to measure these ground motions will yield estimates not only at the permanent borehole station, but at other sites as well.

5.0 REFERENCES

Anderson, J.G., Y.H. Lee, Y.H. Zeng, and S. Day (1996). Control of strong motion by the upper 30 meters, *Bull. Seism. Soc. Am., 86*, 1749-1759.

Atwater, T. (1989). Plate tectonic history of the northeast Pacific and western North America, in *The Geology of North America, Volume N, The Eastern Pacific Ocean and Hawaii*, Winterer E.L., D.M. Hussong, and R.W. Decker (eds.), Geological Society of America, Boulder, 21-72.

Biasi, G.P., and R. Weldon II (1994). Quantitative refinement of calibrated ^{14}C distributions, *Quaternary Res.* 41, 1-18.

Boore, D.M., W.B. Joyner, and T.E. Fumal (1993). Estimation of response spectra and peak accelerations from Western North American earthquakes: An interim report, *U.S. Geol. Surv. Open File Rept., 93-509.*

Borcherdt, R.D., (1994). Estimates of site-dependent response spectra for design (Methodology and Justification), *Earthquake Spectra, 10,* 617-654.

Degenkolb, H.J. and Associates (1978). *Investigation of Seismic Hazards at University of California Campuses*. Consulting report. San Francisco.

Degenkolb, H.J. and Associates (1981). *Seismic Hazard Survey: University of California Buildings*. Consulting report. San Francisco.

Ellsworth, W.L. (1990). Earthquake history, 1769-1989, in *The San Andreas Fault System, California*, R.E. Wallace (Editor), *U.S. Geol. Surv. Prof. Pap. 1515.*

Elrick, S. (1998). Characterization of seismic hazards at the University of California, Riverside, *M.S. Thesis*, University of California, Riverside, California.

Envicom Corporation, and County of Riverside Planning Department, (1976). Seismic safety and safety elements. Technical Report. Riverside, California.

Fumal, T.E., and J.C. Tinsley, (1985). Mapping shear-wave velocities of near surface geologic materials, in *Evaluating Earthquake Hazards in the Los Angeles Region-An Earth-Science Perspective*, J.E. Ziony (Editor), *U.S. Geol. Surv. Prof. Pap., 1360*, 101-126.

Geovision, Inc., (1998). Suspension velocity measurements at the University of California Riverside campus borehole UCR-5, unpublished report # 98257-01.

Gregg In Situ, Inc., (1997). Presentation of cone penetration test data- CLC campus earthquake project, UC Riverside, unpublished report.

Hough, S.E., and E.H. Field (1996). On the coherence of ground motion in the San Fernando Valley, *Bull. Seis. Soc. Am.* 86, 1724-1732.

Jackson, D.D. et al. (1995). Seismic hazards in southern California: Probable earthquakes, 1994 to 2024, *Bull. Seis. Soc. Am.* 85, 379-439.

Joshi, M.S. (1967). The genesis of the granitic and associated rocks of the Box Springs Mountains, Riverside, California, *Ph.D. Thesis*, University of California, Riverside, California.

Lee, T.C., and Hydrogeology and Applied Geophysics Group (1997). *Geophysical Investigation of Subsurface Structures in the Vicinity of March Air Reserve Base*, U.C. Riverside Report for MAFB Project # PCZP970140, 104 pp.

Luetgert, J. (1992). MacRay 1.0.9: Interactive 2-D Seismic Raytracing for the Macintosh, *U.S. Geol. Surv. Open-File Rept.* 92-356, computer disk.

Malinconico, L.L., and T. Larson (1989). *Gravity V1.2*, Micro-innovations, Inc., Carbondale, Illinois.

Matesic, L. and M. Vucetic (1998). *Results of Geotechnical Laboratory Tests on Soil Samples from the UC Riverside Campus*, UCLA research report, ENG-98-198, 208 pp.

Menzie, T.E. (1962). The Geology of the Box Springs Mountains, Riverside County, California, *M.S. Thesis*, Stanford University, Palo Alto, California.

Morton, D.M., and B.F. Cox (1988). Geologic map of the Riverside East Quadrangle, Riverside County, Calfornia, *U.S. Geol. Surv. Open-File Rept.* 88-754.

Morton, D.M., and J.C. Matti (1987). The Cucamonga fault zone: geologic setting and Quaternary history, *U.S. Geol. Surv. Prof. Pap. 1339*, 179-203.

Morton, D.M., and J.C. Matti (1993). Extension and contraction within an evolving divergent strike-slip fault complex: the San Andreas and San Jacinto fault zones at their convergence in southern California, in *The San Andreas Fault System: Displacement, Palinspastic Reconstruction, and Geologic Evolution*, Powell, R.E., R.J. Weldon II, and J.C. Matti (eds.), *Geol. Soc. Am. Memoir 178*, 217-230.

Nelson, J.W., R.L. Pendleton, J.E. Dunn, A.T. Strahorn, and E.B. Watson (1917). *Soil Survey of the Riverside Area, California*, U.S. Dept. Agriculture, Washington, 88 pp.

Park, S.K., D. Pendergraft, W.J. Stephenson, K.M. Shedlock, and T.C. Lee (1995). Delineation of intrabasin structure in a dilational jog of the San Jacinto fault zone, southern California, *J. Geophys. Res.* 100, 691-702.

Park, S.K., and S. Elrick (1998). Predictions of shear-wave velocities in southern California using surface geology, *Bull. Seism. Soc. Am.*, 88, 677-685.

Pearson, D.C. (1994). Integrated study of full wave-field seismic site characterization techniques: data acquisition, wave-field generators, and full wave-field, constrained inversion of surface refraction data, *Ph.D. Dissertation*, Southern Methodist University, Dallas, Texas.

Petersen, M.D., and S.G. Wesnousky, (1994). Fault slip rates and earthquake histories for active faults in southern California, *Bull. Seis. Soc. Am.* 84, 1608-1649.

Powell, R.E. (1993). Balanced palinspastic reconstruction of the pre-Late Cenozoic paleogeology, southern California: Geologic and kinematic constraints on evolution of the San Andreas fault system, in *The San Andreas Fault System: Displacement, Palinspastic Reconstruction, and Geologic Evolution*, Powell, R.E., R.J. Weldon II, and J.C. Matti (eds.), *Geol. Soc. Am. Memoir 178*, 1-106.

Press, W.H., S.A. Teukolsky, W.T. Vetterling, and B.P. Flannery, (1992). *Numerical Recipes in Fortran* Cambridge Univ. Press, New York, 963 pp.

RimRock Geophysics (1995). *User's Guide to SIP Shell*, RimRock Geophysics, Inc., Englewood, Colorado.

Robertson P.K., and R.G. Campanella, (1988). *Guidelines for Use, Interpretation, and Application of the CPT and CPTU*, Hogentogler and Co., Gaithersburg, Maryland.

Rockwell, T.K., E.M. Gath, and T. Gonzalez (1992). Sense and rate of slip on the Whittier fault zone, eastern Los Angeles basin, in *Proc. of the 35th Annual Meeting Association of Engineering Geologists October 2-9, 1992*, M.L. Stout (ed.), 679.

Rockwell, T.K., R. Klinger, and J. Goodmacher (1990). Determination of slip rates and dating of earthquakes for the San Jacinto and Elsinore faults, in *Geology around the Margins of the Eastern San Bernardino Mountains*, M.A. Kooser and R.E. Reynolds (eds.), Inland Geological Society, Redlands, 51-56.

Rockwell, T.K., R.S. McElwain, D.E. Millman, and D.L. Lamar (1986). Recurrent late Holocene faulting on the Glen Ivy North Strand of the Elsinore fault at Glen Ivy Marsh, in *Guidebook and Volume on Neotectonics and Faulting in Southern California, Cordilleran Section, Geological Society of America*, 167-1275.

Sanders, C. and H. Magistrale, (1997). Segmentation of the northern San Jacinto fault zone, southern California, *J. Geophys. Res.*, 102, 27453-27467.

Sieh, K. (1986). Slip rate across the San Andreas faults and prehistoric earthquakes in Indio, California, *EOS* 67, 1200.

Sieh, K., M. Stuiver, and D. Brillinger (1989). A more precise chronology of earthquakes produced by the San Andreas fault in southern California, *J. Geophys. Res.*, 94, 603-623.

Telford, W.M., L.P. Geldart, and R.E. Sheriff (1990). *Applied Geophysics*, 2nd Ed., Cambridge University Press, New York.

Tinsley, J.C., and T.E. Fumal, (1985). Mapping Quaternary sedimentary deposits for areal variations in shaking response, in *Evaluating Earthquake Hazards in the Los Angeles Region-An Earth-Science Perspective*, J.E. Ziony (Editor), *U.S. Geol. Surv. Prof. Pap., 1360*, 101-126.

Todd, V.R., B.G. Erskine, and D.M. Morton (1989). Metamorphic and tectonic evolution of the northern Peninsular Ranges batholith, southern California, in *Metamorphism and Crustal Evolution of the Western United States*, Ernst, W.G. (ed.), Prentice Hall, Englewood Cliffs, 894-937.

Welenco, Inc., (1998). Geophysical logs for UC Riverside hole UCR-5, unpublished.

Wesnousky, S.G. (1986). Earthquakes, Quaternary faults, and seismic hazard in southern California, *J. Geophys. Res.* 91, 12587-12632.

WGCEP (Working Group on California Earthquake Probabilities) (1988). Probabilities of large earthquakes occurring in California on the San Andreas fault, *U.S. Geol. Surv. Open-File Rept. 88-938*.

Woodford, A.O., J.S. Shelton, D.O. Doehring, and R.K. Morton (1971). Pliocene-Pleistocene history of the Perris block, southern California, *Geol. Soc. Am. Bull.* 82, 3421-3448.

Zawila, J.S. (1997). Gravity mapping of subsurface structures in the central Perris tectonic block, southern California, *M.S. Thesis*, University of California, Riverside, California.

6.0 ACKNOWLEDGMENTS

This project would not have been possible without Michael Webster, Vice Chancellor of Administration, whose awareness of the seismic hazards at UCR led him to support this work. While this report was written by the PI from U.C. Riverside and his two students, a much larger group of scientists contributed to the work presented herein. Francois Heuze and Jeff Wagoner, both from Lawrence Livermore National Laboratory, provided extensive editorial assistance as well as assistance during the installation of the seismic station. Francois Heuze, as chief scientist of the Campus Earthquake Program, provided guidance throughout, the photos in Figures 17 and 25-27, and Figure 30. Craig Pearson, from Los Alamos National Laboratory, loaned to our Program the shear-wave generator which he had designed and built. Jamie Steidl, from U.C. Santa Barbara, provided assistance during the station installation and later supplied the records of the October 1998 earthquakes. The other campus PIs, Ralph Archuleta (UCSB), Bernard Minster (UCSD), and Mladen Vucetic (UCLA), contributed many valuable discussions. Egill Hauksson and CalTech provided their technical expertise in connecting our seismic station to their Trinet network and loaned UCR a second data acquisition unit in return for permission to archive the data. Frank Vernon (UCSD) set up a parallel data logging site in San Diego. All of this permits the UCR PI to avoid having to set up an independent data archival system, and *that* is gratefully acknowledged!